THE UNIVERSITY OF MICHIGAN RESEARCH INSTITUTE
ANN ARBOR

AN APPROACH TO FREQUENCY IDENTIFICATION IN FAST-SCANNING PANORAMIC RECEIVERS

Technical Report No. 110

Cooley Electronics Laboratory
Department of Electrical Engineering

By: D. W. Fife

Approved by: A. B. Macnee
A. B. Macnee

Project 2899

TASK ORDER NO. EDG-3
CONTRACT NO. DA-36-039 sc-78283
SIGNAL CORPS, DEPARTMENT OF THE ARMY
DEPARTMENT OF ARMY PROJECT NO. 3A 99-06-001-01

July 1960

Eugene
UHR
1460

TABLE OF CONTENTS

LIST OF ILLUSTRATIONS

LIST OF ILLUSTRATIONS (Continued)

ABSTRACT

This report discusses a self-adaptive, programmed-sweep receiver for signal frequency identification in panoramic receiver applications requiring low search time. The design problems are explained. Feasibility of the programmed-sweep receiver is shown for a simple model of a two-scan receiver.

AN APPROACH TO FREQUENCY IDENTIFICATION IN FAST-SCANNING PANORAMIC RECEIVERS

1. INTRODUCTION

The peak output response of a fast-scanning panoramic receiver to CW signals varies inversely as the square root of the sweep rate, while the output pulse width is the same as the width of the impulse response of the IF filter (Ref. 1). Hence, in fast-scanning receivers the effective output signal-to-noise ratio goes down as the sweep rate increases.

Many applications of panoramic receivers require fast sweeping in order to achieve a quick reaction to signals which may appear suddenly. It becomes clear, however, that a sweeping receiver with an automatic frequency control for locking-on at the frequency of the received signal may not be able to acquire a weak signal as a result of the decreased output signal-to-noise ratio due to fast sweeping.

It is therefore of interest to consider different techniques for obtaining frequency information automatically. This report discusses a programmed-sweep panoramic receiver which acquires the frequency of a received signal by scanning a progressively-smaller band enclosing the signal frequency. The receiver makes as many sweeps as necessary to locate the signal frequency within some preselected bandwidth, which might be the bandwidth of the IF filter.

By the choice of a simple model of the programmed-sweep receiver, some numerical results have been obtained for the two-scan case. These results are compared with corresponding data for a receiver which makes one scan in the same time interval. The advantage of the programmed-sweep receiver for the two-scan case is thereby demonstrated.

2. PANORAMIC RECEIVER SIMULATION

Experimental studies of panoramic receivers have been carried on at this laboratory using equipment known as SIMRAR (SIMulated Receiver And Recorder). This equipment simulates an IF amplifier, detector (linear or nonlinear), and gated video amplifier and includes suitable threshold and recording devices for obtaining the statistical properties of the receiver output. By applying at the IF amplifier input suitable signals and noise, SIMRAR can be used to study signal detection with a variety of receivers, including a panoramic receiver.

The use of SIMRAR in panoramic receiver experiments has been described in detail in a previous report (Ref. 2), so only a basic description is given here. Figure 1 is the block diagram of the equipment. For the present study, the diode function generator has been used to obtain a square law detector characteristic, and a video filter with a bandwidth of 40 cps has been used.

An auxiliary signal generator (Ref. 2) provides a panoramic signal which linearly sweeps in frequency from approximately 300 to 3000 cps. Timing circuits in SIMRAR apply this signal to the IF amplifier input on alternate detection trials. Thus, SIMRAR alternately makes trials with signal-and-noise present and noise alone present. The

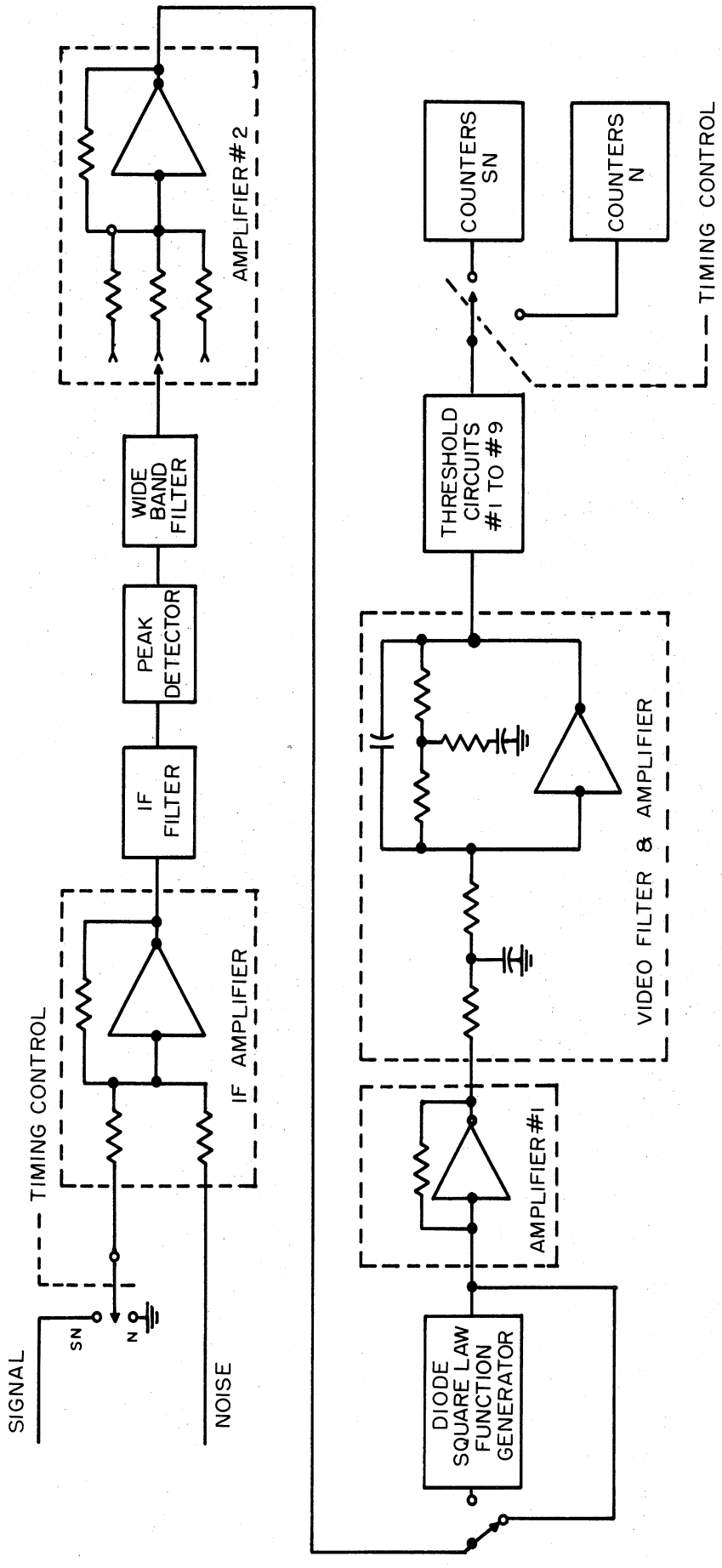

FIG. 1 SIMRAR AS USED IN PANORAMIC RECEIVER TESTING

timing circuits also control the length of the observation time interval, which can be preset over a wide range, and the two banks of counters which record the amplitude distribution of the receiver output for the signal-and-noise and noise alone alternatives. After a sufficiently large number of trials (500 to 1000 per alternative) the counters yield estimates of the probabilities,

$P_{SN}(A)$ = probability of detection, and

$P_{N(A)}$ = probability of false alarm,

for the decision threshold value which has been preset for each threshold detector circuit. The probabilities from each of the nine counter pairs are plotted on normal-normal probability paper to obtain the receiver operating characteristic (ROC).

Table I gives the range of parameter variation which can readily be obtained with this equipment. The parameters of interest are defined as follows:

b = IF filter bandwidth (rad/sec) = 44π,

s = receiver sweep speed (rad/sec^2),

B_o = frequency band swept by the receiver on the initial scan (rad/sec) = sT_o, where

T_o = observation time interval (sec),

$\frac{S}{N}$ = peak signal-to-noise power ratio measured at IF filter output (dimensionless).

TABLE I

RANGE OF PARAMETER VARIATION IN

RECEIVER SIMULATION

Parameter	Range
Signal-to-Noise Power Ratio $\frac{S}{N}$	3.3 - 18.2
Normalized Sweep Rate s/b^2	0.15, 0.3, 0.5, 1.2, 2.0
Normalized Sweep Bandwidth B_o/b	10 - 100
Detectability Index d'	0.2 - 4.0

The signal-to-noise power ratio $(\frac{S}{N})$ defined here is found by measuring the signal power with a true rms meter at the IF filter output, with the signal frequency constant and equal to the IF filter center frequency. $\frac{S}{N}$ is the ratio of this power and the noise power measured at the same point. $\frac{S}{N}$ is varied by changing the resistor at the IF amplifier input to attenuate the signal. The noise source is set to give a constant IF filter output of 5.5 volts rms.

The parameter d' is a measure of signal detection performance (Ref. 3). In general, each point on an ROC (corresponding to a particular value of decision threshold) has a different value of d'. However,

if the ROC is normal (at a 45° angle) the d' value of the point on the ROC with equal conditional errors becomes a singular measure of the signal detection performance of the receiver. Figure 2 is an example of a normal ROC.

In the study of the frequency identification problem an additional circuit was employed with the receiver simulation. This is a holding circuit, the block diagram of which is shown in Fig. 3. In this application the holding circuit has two outputs, one of which is the peak value of the video amplifier output on one scan. The other is a voltage which is proportional to signal frequency and which is clamped at the instant the maximum output occurs. These outputs were used to drive the vertical and horizontal deflection systems of an oscilloscope. Photographic records were thereby obtained over a large number of receiver sweeps. A schematic diagram of the holding circuit is given in Appendix A as also is a detailed description of its operation.

3. THE PROGRAMMED-SWEEP RECEIVER

The purpose of the programmed-sweep panoramic receiver is to search a given frequency band and detect the presence and identify the frequency of received signals. An improvement over the performance of a single-scan receiver is desired. To be consistent with the applications of a fast-scanning receiver, frequency identification should be accomplished as soon as possible after the signal appears.

The evaluation of panoramic receiver operating characteristics and the influence of the receiver design, insofar as signal detection

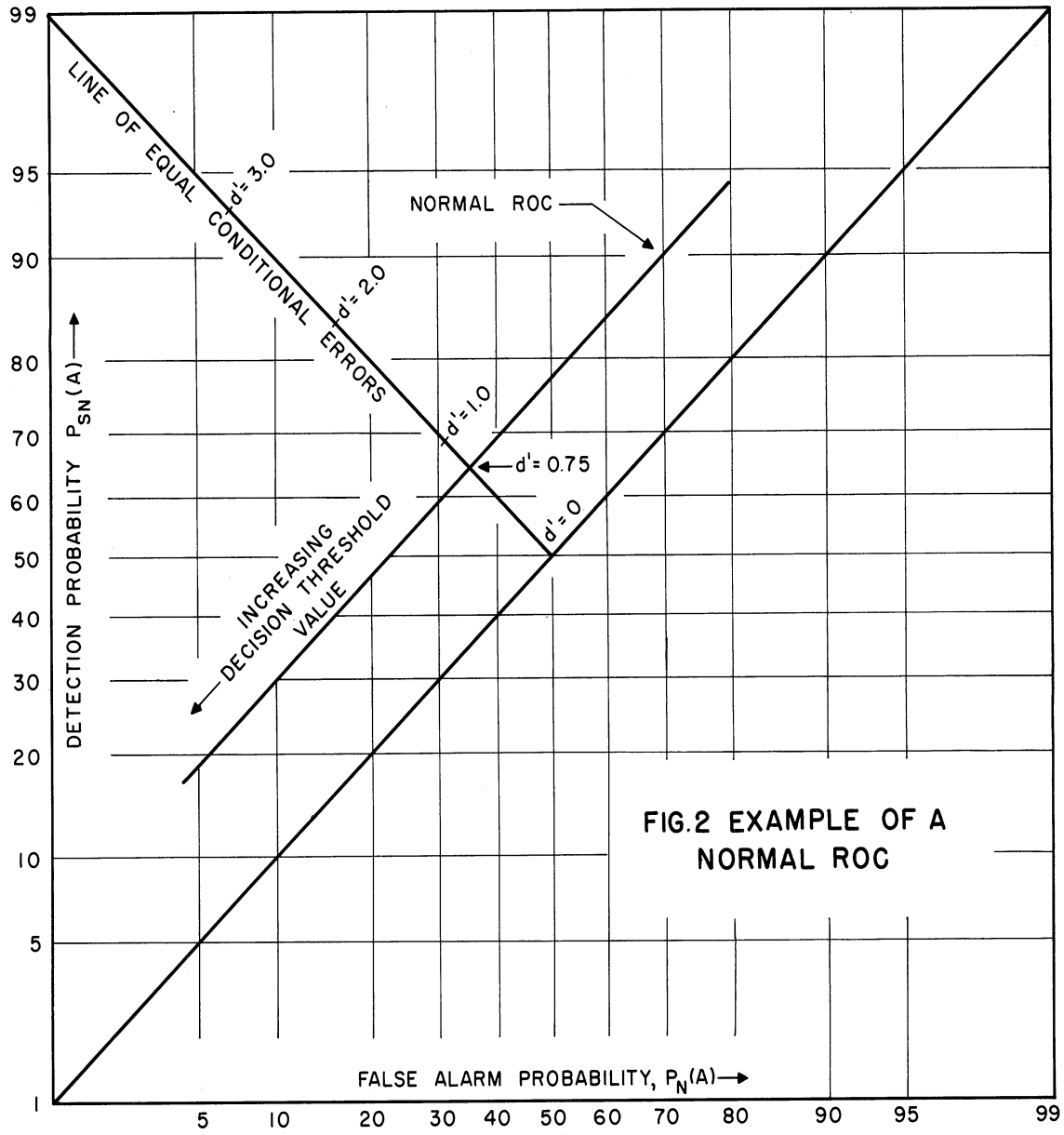

FIG.2 EXAMPLE OF A NORMAL ROC

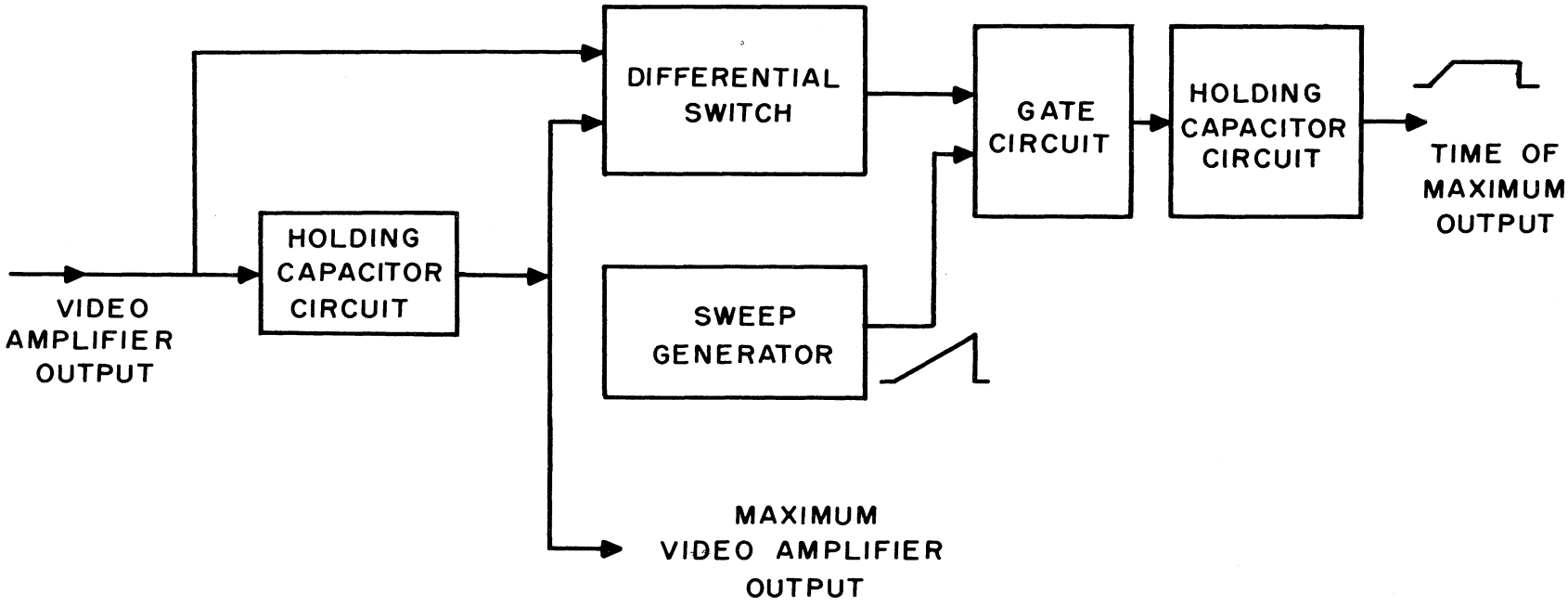

FIG. 3 BLOCK DIAGRAM OF HOLDING CIRCUIT

on the initial scan is concerned, have already been described (Ref. 2). In this section the general aspects of the frequency identification problem are discussed.

Figure 4 contrasts the outputs of slow- and fast-scanning receivers on the initial scan past the frequency of a CW signal. Since the signal response is much larger than the noise level in the slow-scanning receiver, the signal frequency is easily identified on the initial scan as the frequency at which maximum output occurs. (All time lags due to filtering, etc., are neglected here. It is assumed that the peak response to the signal occurs at the signal frequency.) For the fast-scanning receiver, however, the maximum output will not, in general, occur at the signal frequency. Indeed, the difference between the true signal frequency and the frequency of maximum output, B_D, is a random variable. Its probability distribution function depends upon the sweep rate, sweep time, input signal-to-noise ratio, and the value of the maximum output amplitude.

To obtain a qualitative understanding of the joint distribution of the maximum output amplitude per scan, and the difference between the true signal frequency and the frequency of maximum output, photographs were taken utilizing the one-scan panoramic receiver simulation. These are shown in Figs. 5 through 9. Each spot on these photographs records the maximum output amplitude and the frequency at which it occurred for one scan. The true signal frequency is located at the center of each photograph. Each photograph records approximately 500 scans with signal present.

The photographs show that the difference frequency, B_D,

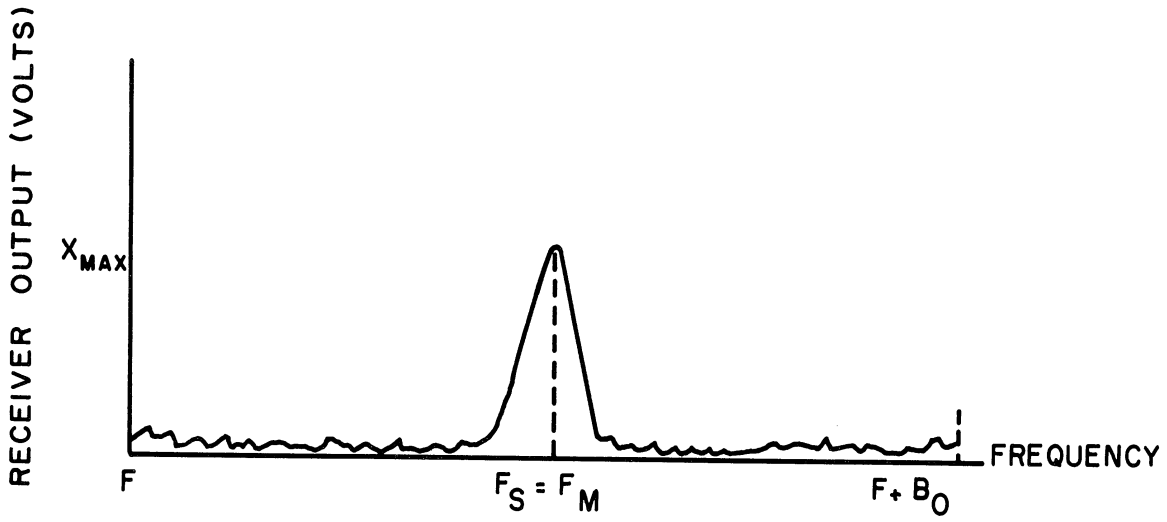

(a) SLOW SCANNING RECEIVER

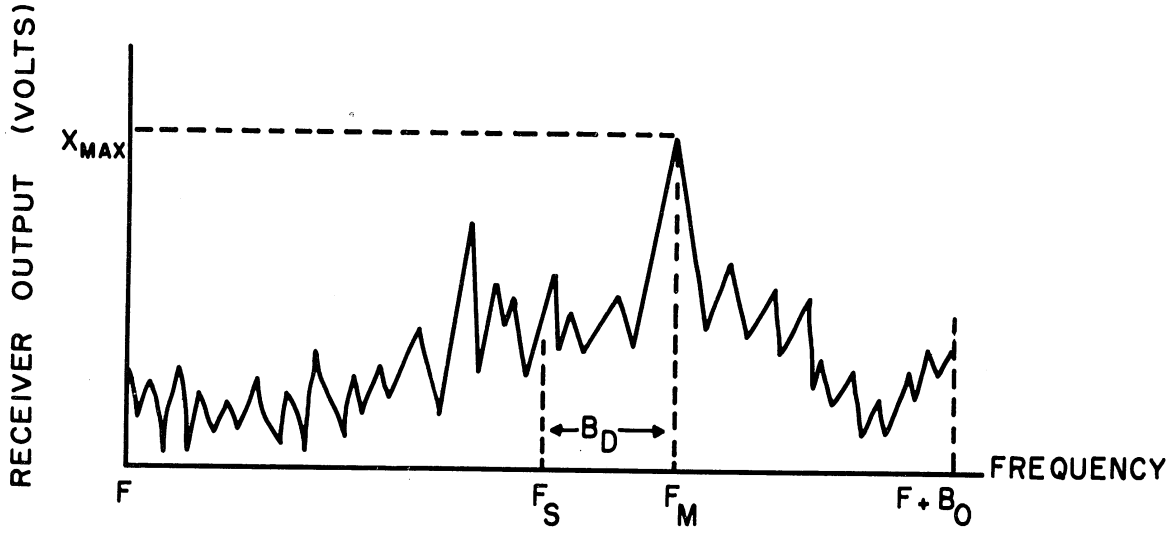

(b) FAST SCANNING RECEIVER

FIG. 4 POSSIBLE RECEIVER OUTPUT WAVEFORMS WITH CONSTANT INPUT SIGNAL-TO-NOISE RATIO

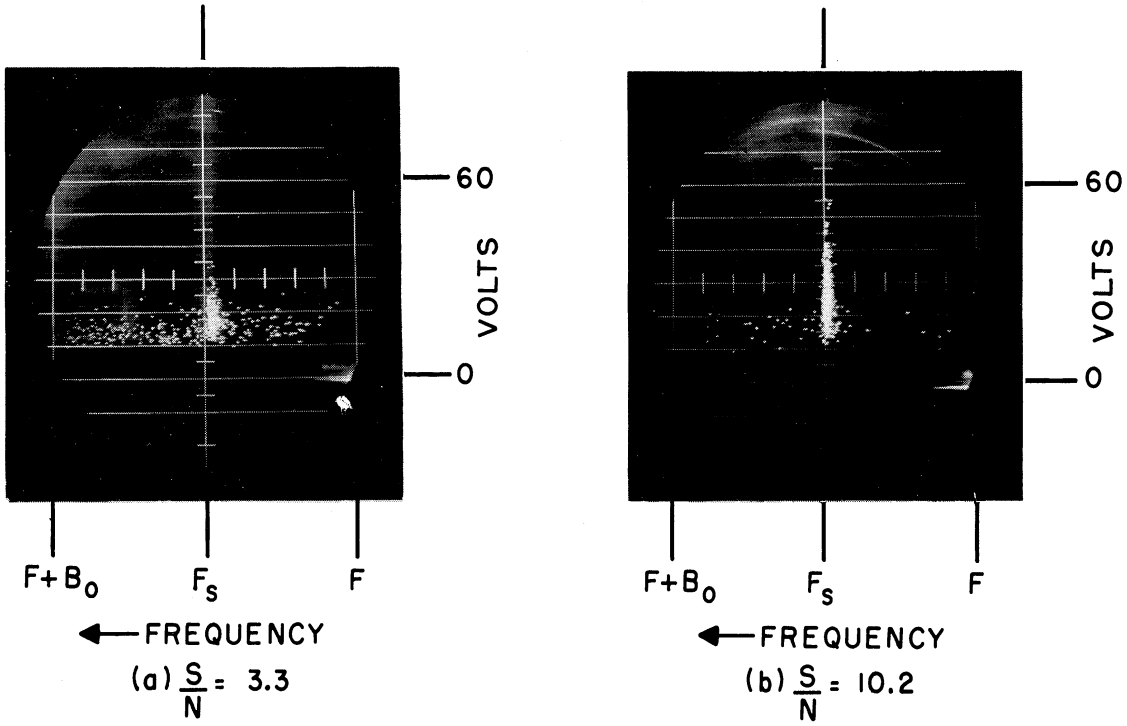

FIG. 5 MAXIMUM RECEIVER OUTPUT AMPLITUDE VERSUS FREQUENCY, $B_0 = 100b$, $\frac{s}{b^2} = 0.5$

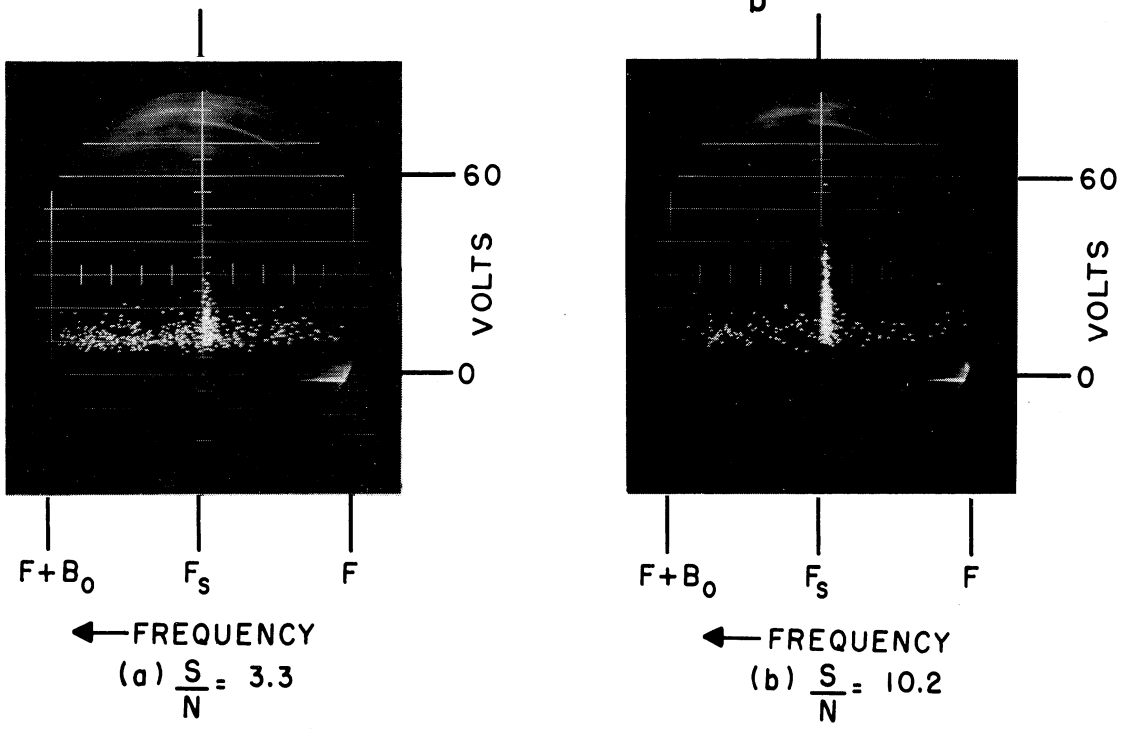

FIG. 6 MAXIMUM RECEIVER OUTPUT AMPLITUDE VERSUS FREQUENCY, $B_0 = 100b$, $\frac{s}{b^2} = 1.2$

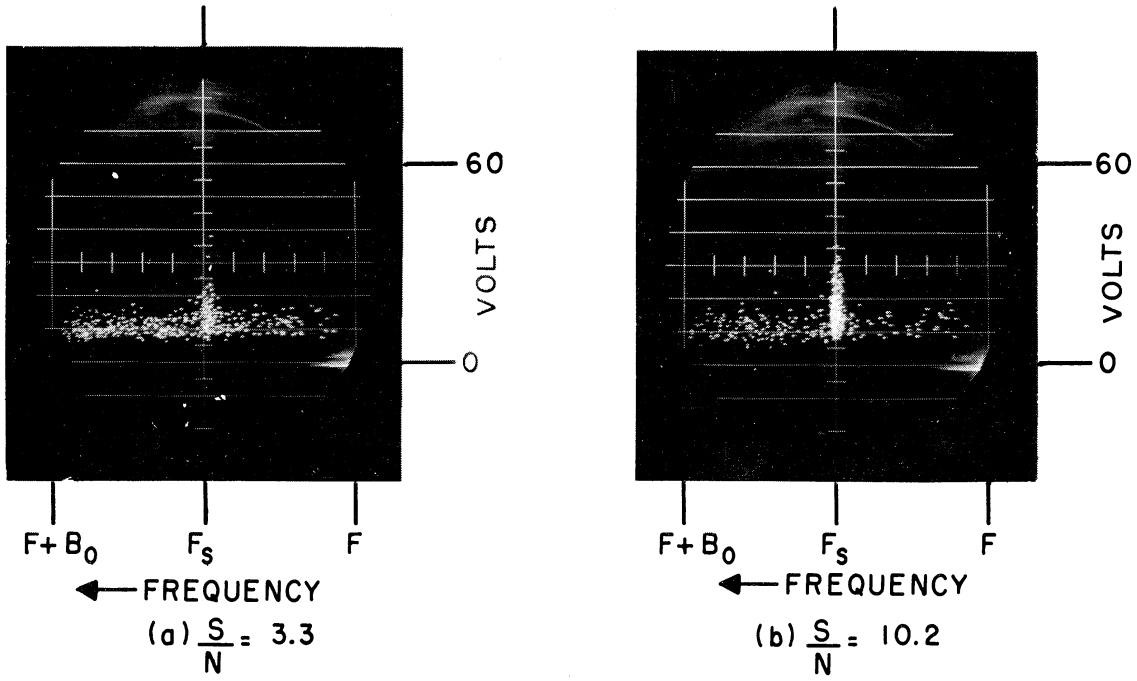

FIG. 7 MAXIMUM RECEIVER OUTPUT AMPLITUDE VERSUS FREQUENCY, $B_0 = 100b$, $\frac{S}{b^2} = 2$

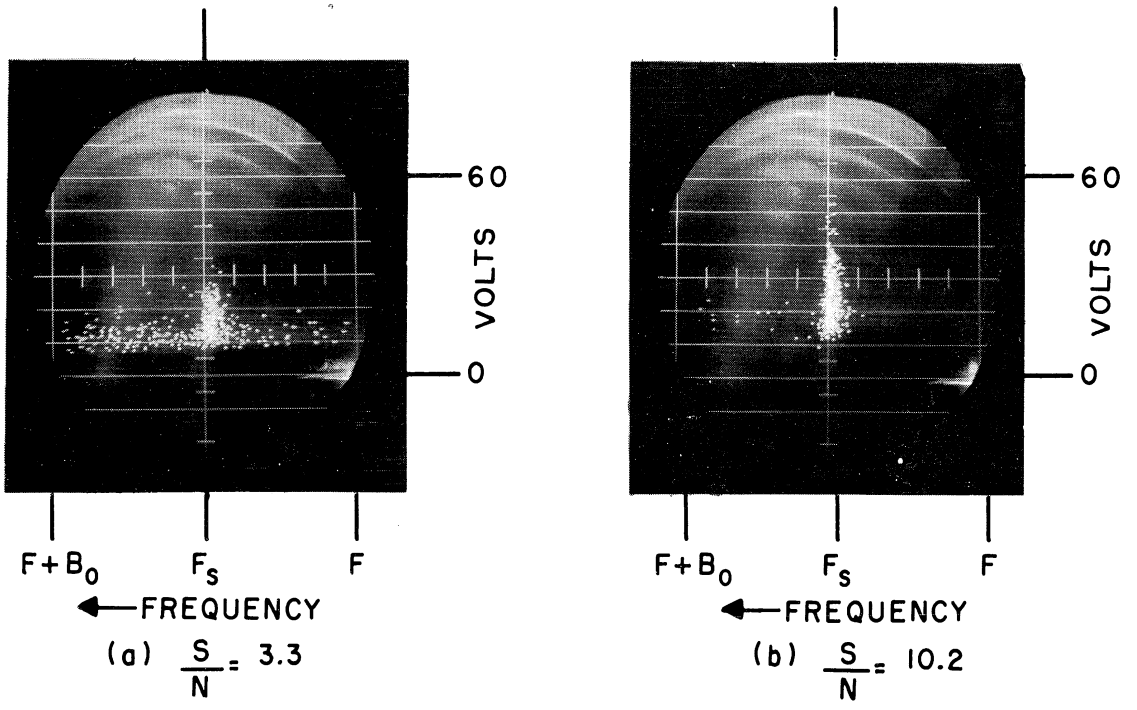

FIG. 8 MAXIMUM RECEIVER OUTPUT AMPLITUDE VERSUS FREQUENCY, $B_0 = 25b$, $\frac{S}{b^2} = 0.3$

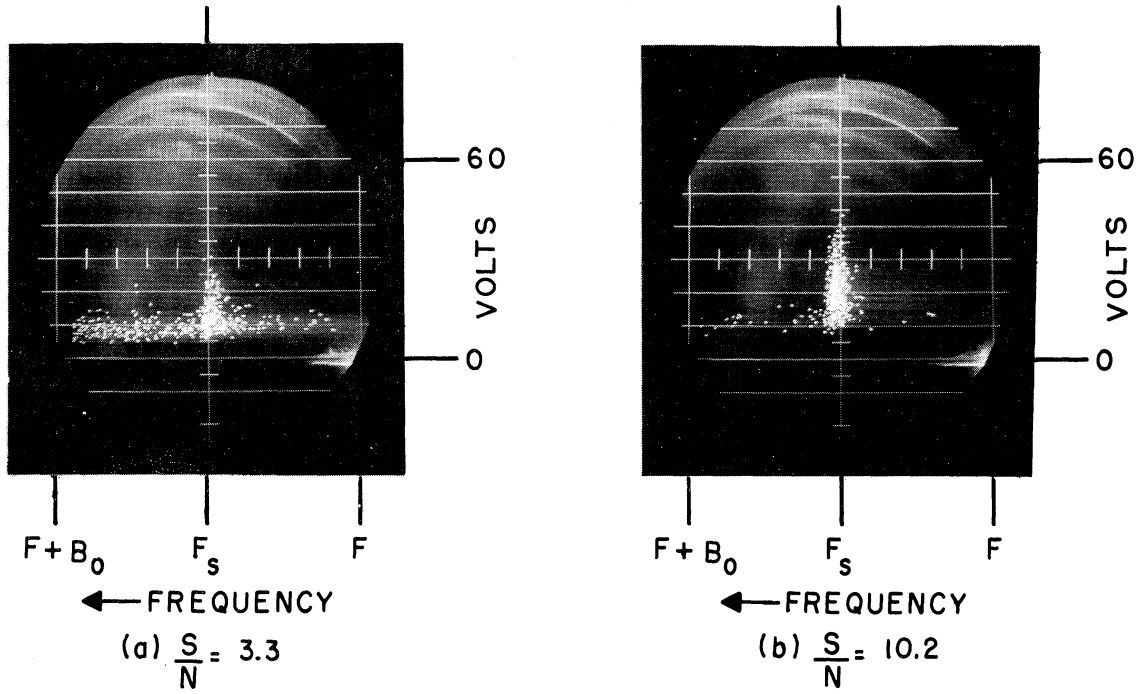

Fig. 9. Maximum Receiver Output Amplitude Versus Frequency, $B_o = 25b$, $\frac{s}{b^2} = 0.5$

is statistically dependent upon the maximum output amplitude. The expected frequency difference is small for large amplitudes, becoming larger as the maximum amplitude decreases, until at the lowest amplitudes recorded a frequency difference of half the band swept may often occur. These effects are clearly seen by comparing photographs for high and low S/N cases or high and low s/b^2 cases. Notice that at low amplitudes the spread of points is not uniform across the band swept; there is still a tendency for the difference frequency to be relatively small.

From consideration of photographs of this kind, it is possible to obtain a functional relationship between the maximum receiver output, x_{max}, and the frequency difference, B_o, which satisfies approximately some probability condition at constant S/N and s/b^2. For example, the curve of Fig. 10a might be such a function. Fig. 10b

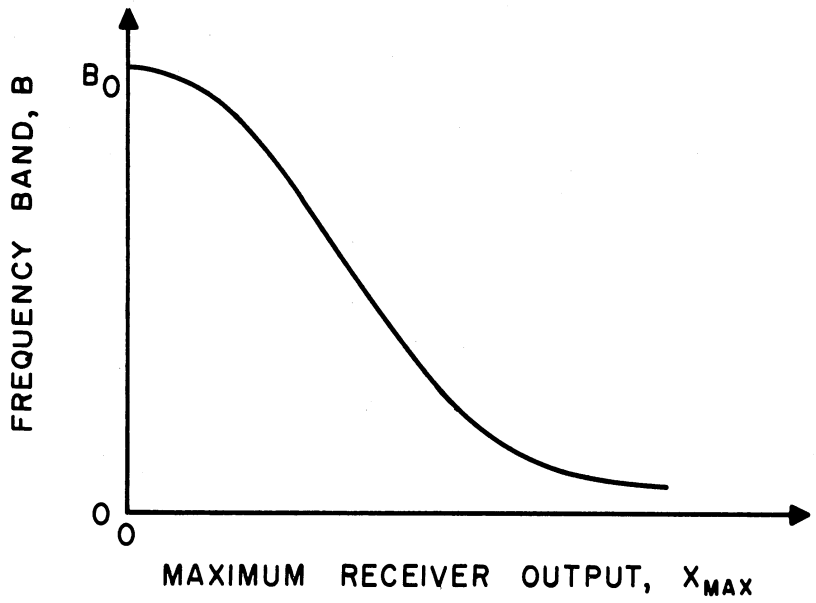

(a) FUNCTION $B = f(X_{MAX})$

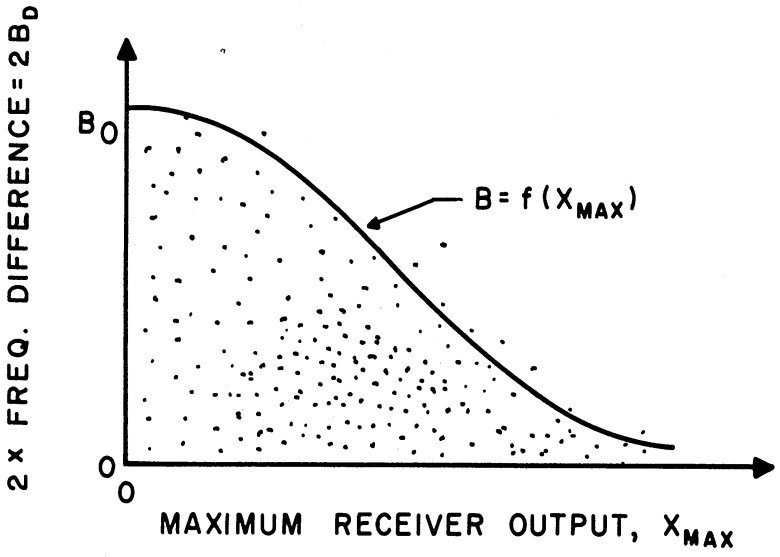

(b) RELATIONSHIP OF FUNCTION TO RECEIVER OUTPUT POINTS OVER LARGE NUMBER OF SWEEPS

FIG.10 EXAMPLE OF A FUNCTION FOR WHICH $P_{X_{MAX}}(B_D \leq B)$ HAS A GIVEN VALUE ON A SINGLE SWEEP

indicates how this is obtained from photographs such as Figs. 5 through 9. Then by instrumenting the function in a receiver, it is possible to obtain from the maximum amplitude on a single scan a frequency band, centered on the frequency of maximum output, such that there exists a given probability that the true signal frequency is located in this band. Furthermore, by requiring only that the signal frequency be located within the band with a probability at least as large as some value, a function can be chosen which is applicable for all sweep rates and signal-to-noise ratios. This function will be called a sweep-program function for the receiver.

A technique of frequency identification can now be described.

(1) On each sweep of the receiver, the maximum output amplitude determines, by means of a program function, a frequency band within which the signal frequency is likely to be.

(2) The next scan of the receiver is the band determined by the previous sweep, but at a lower sweep rate. The maximum output amplitude expected will be larger, so the band determined on this scan is expected to be smaller than before. Thus, over a number of scans, the band swept will gradually converge on the signal frequency.

(3) The receiver continues sweeping until the frequency band determined by the program function is smaller than some preselected bandwidth. By proper choice of this condition, the true signal frequency is identified within some desired maximum error. In many cases, the desired maximum error is the bandwidth of the IF filter.

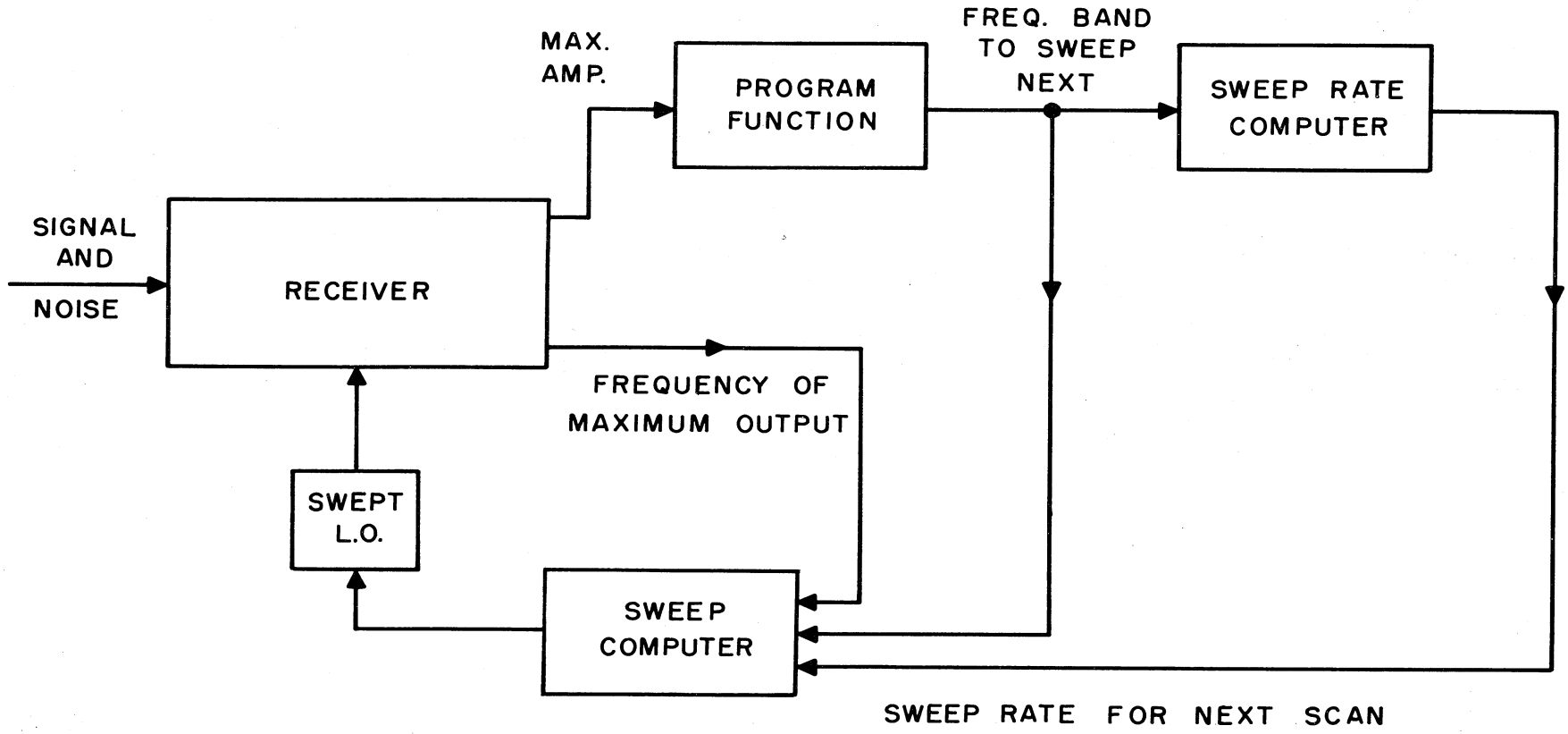

FIG. 11 BLOCK DIAGRAM OF A PROGRAMMED-SWEEP PANORAMIC RECEIVER

A block diagram, depicting the general form of the instrumentation for this technique, is shown in Fig. 11. For a particular choice of program function, a possible pattern of the frequency-time sweep of the receiver is shown in Fig. 12.

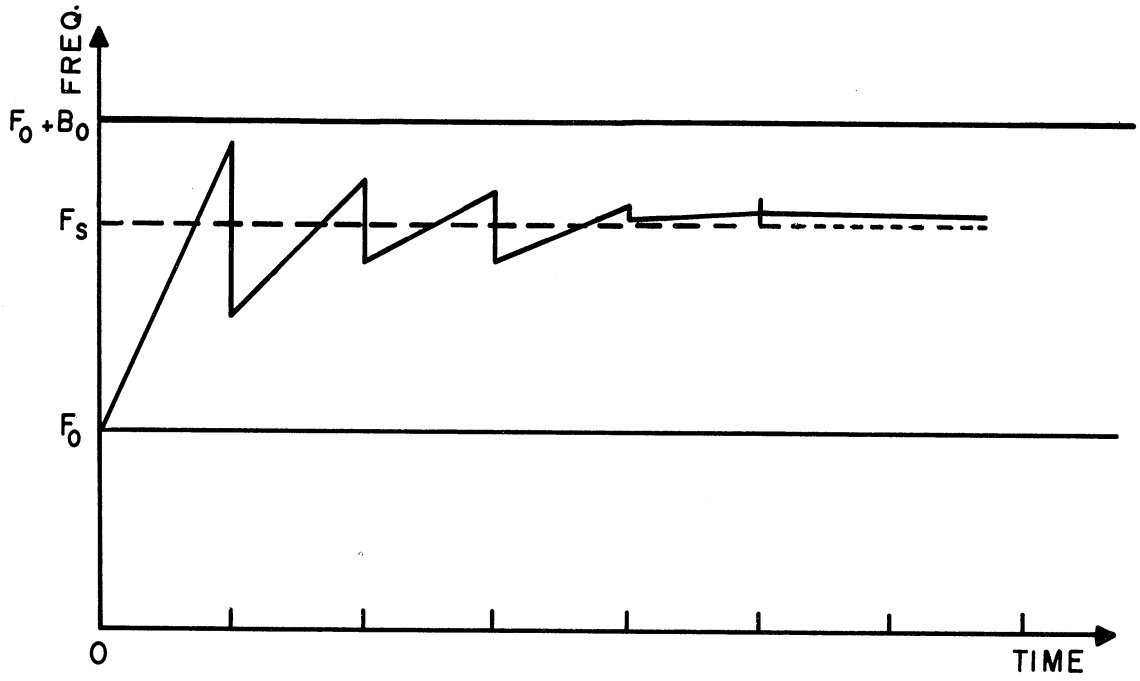

Fig. 12. Possible Frequency-Time Sweep Pattern of a Programmed-Sweep Panoramic Receiver

It should be emphasized that in application of this technique the desired performance is:

(1) If no signal is present, the receiver continues to search the entire band (no convergence on noise).

(2) The receiver will correctly identify the frequency of a received signal (correct identification).

(3) Correct frequency identification is accomplished in minimum time (minimum identification time).

However, since the frequency identification technique basically involves

operations on a random process, this desired performance can only be approached with practical equipment. A discussion of the statistical quantities and features of the receiver instrumentation which affect the performance is given below.

Figure 10 shows one form of a program function. For this form, the maximum receiver output determines an absolute frequency band for the next sweep. Another form for a program function would be such that the maximum amplitude determines a frequency band for the next sweep relative to the band of the present sweep. In other words, the maximum output on one sweep determines what portion of the band swept should be rescanned. Consider for the moment that a receiver uses this form of program function.

Suppose that on one particular sweep after frequency identification has begun the receiver should fail to intercept the signal, i.e., fail to sweep through the signal frequency. Then after this sweep, if the receiver continues to sweep a portion of the band swept previously, the result is incorrect, since effectively all information regarding the true signal frequency has been lost. But, in addition, the expected maximum amplitudes are relatively small, since observation is made primarily on noise with, at most, a small part of the total signal response. Then, a way to overcome the difficulty of an intercept failure is to design the program function such that if the maximum amplitude is below a chosen threshold, the next sweep of the receiver is the initial frequency band. Thus, when interception fails, the frequency identification process starts over. The general program function described is depicted in Fig. 13.

Note that if X_c is the threshold value for the signal detection

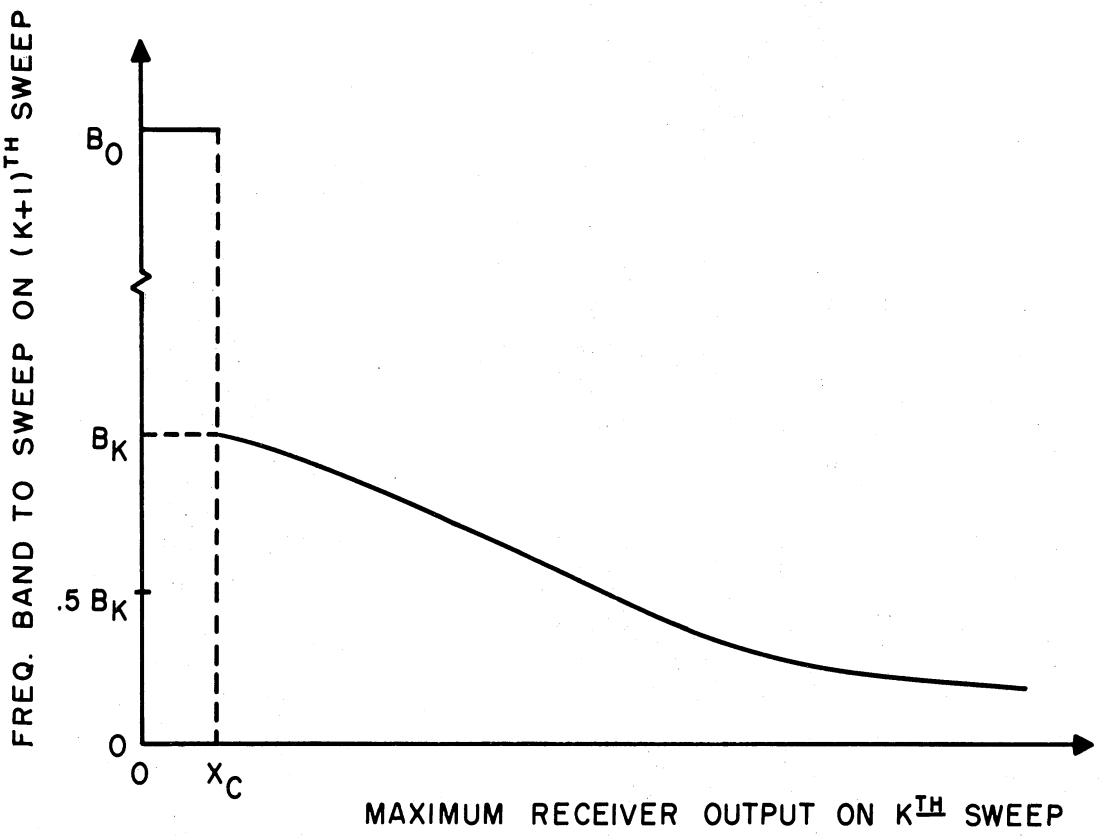

Fig. 13. Form of a Program Function Defining a Relative Rescan Band

decision, the program function of Fig. 13 effectively tests the hypothesis, "signal present," on every sweep of the receiver. Furthermore, the receiver does not begin converging on the signal frequency until a detection of the signal occurs.

Using Fig. 14 it can be shown that the relative band type of program function is more desirable than the absolute band type insofar as the rate of convergence on the signal frequency is concerned. Suppose the receiver has completed the kth scan in the frequency identification process. The band swept, B_k, was determined by X_{k-1}, the maximum amplitude on the (k-1)th scan. Now, in order for B_{k+1} to be less than B_k, X_k must be greater than X_{k-1} for the absolute band function, but X_k need only be greater than X_c, the decision threshold value, for the relative band function. The probability $P(X_k > X_c)$

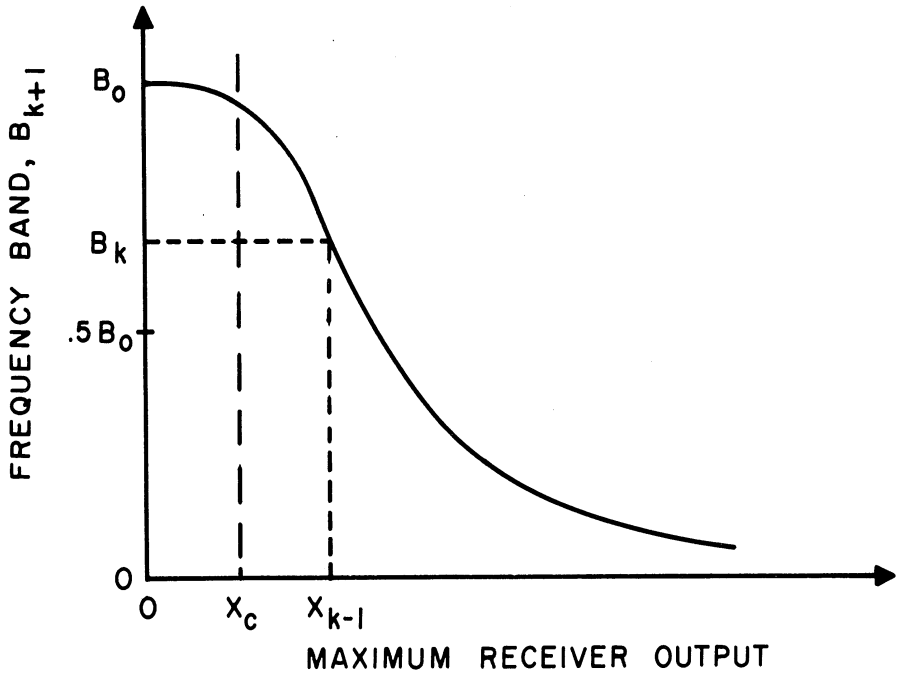

(a) PROGRAM FUNCTION, ABSOLUTE BAND

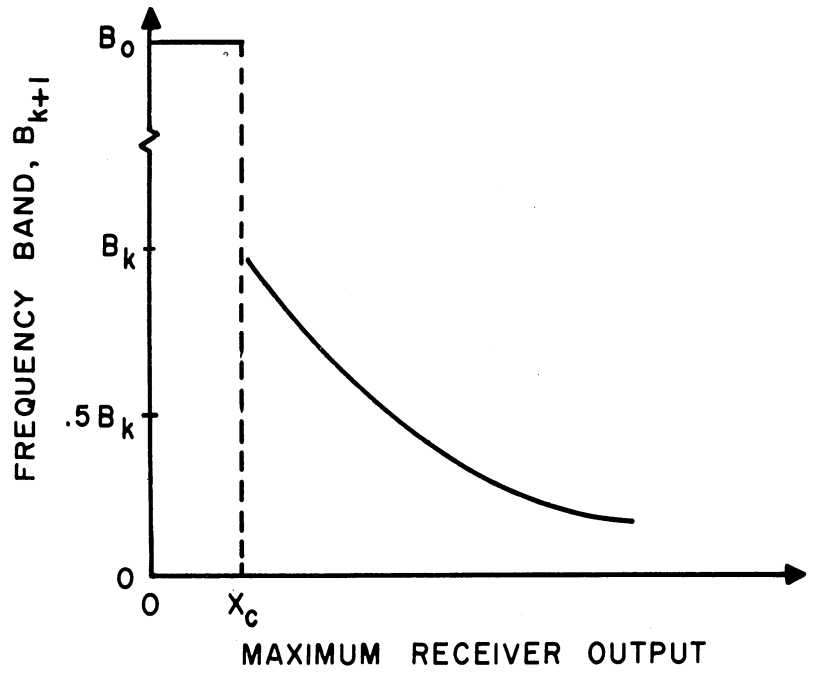

(b) PROGRAM FUNCTION, RELATIVE BAND

FIG.14 COMPARISON OF PROGRAM FUNCTION TYPES

is greater than $P(X_k > X_{k-1})$ for all $X_{k-1} > X_c$. Hence, on any sweep, it is more probable that the relative band function will yield a smaller band, unless a miss ($X_{k-1} < X_c$) occurs on the previous sweep. Once convergence on the signal frequency has begun, the miss probability diminishes rapidly since the sweep speed is decreasing. Before convergence on the signal frequency begins, i.e., before detection of the signal occurs, the absolute band function yields sweep bandwidths which are only somewhat less than B_o and hence does not really present an advantage over the relative band function.

The program function of Fig. 13 will also reduce convergence on noise. If a signal is not present, a detection decision is a false alarm. Since frequency identification does not begin until a detection decision is made, convergence on noise depends first upon the false alarm probability, which in turn depends upon the noise power, sweep time, and decision threshold value. If the false alarm probability on one scan is constant, the probability that a false alarm will occur on each of k consecutive scans is the kth power of the false alarm probability on one scan. This diminishes quite rapidly if the one-scan false alarm probability is small. Hence, if the decision threshold value is chosen to yield a fairly small false alarm probability on one scan, the receiver will attempt only a few scans in the frequency identification with no signal present before the sweep reverts to the original band.

It is desired that frequency identification be accomplished in minimum time. The identification time can be written

$$T_I = \sum_{i=1}^{n} T_i = \sum_{i=1}^{n} B_i/s_i, \qquad (1)$$

where T_i is the time required for the ith scan after the first detection, and n is the total number of scans required after the first detection for correct identification. Now, n is comprised of k consecutive scans on each of which the signal is detected and which result in correct frequency identification, and all additional scanning after the first detection which results in a detection failure.

A detection failure will occur if the signal is not intercepted or if the maximum receiver output as it sweeps through the signal frequency is not sufficient to exceed the decision threshold. Hence, it would appear that to minimize T_I, both the probability of intercept and probability of correct signal detection should be as high as possible. But, in order to have the intercept probability arbitrarily close to unity, the band swept on every scan should be the band swept on the initial scan. Certainly no progress is made toward frequency identification if this is true. Also, for constant decision threshold value and band swept, the probability of correct signal detection increases as the sweep rate decreases. But as the sweep rate becomes very small, the scan time and, hence, the identification time, becomes very large.

It appears, then, that the choice of a program function and sweep rate computer to yield minimum identification time must represent an optimum relationship between intercept probability, detection probability, scan time, and total number of scans. Determination of the program function and the related sweep rate computer is the design problem for the programmed-sweep panoramic receiver. An analytical approach to a solution appears to be out of the question, since a mathematical expression for the statistics of the receiver output as a function of sweep rate, signal-to-

noise ratio, and sweep time is not available. An experimental solution is beyond the scope of the present work.

The question of the feasibility of the programmed-sweep receiver as a means of frequency identification has not been considered up to this point. Clearly, a certain number of scans will be required to correctly identify the frequency of most of the signals received. It remains to be shown that frequency resolution cannot be equally-well achieved in the same time by making one slow sweep of the receiver. Although this is difficult to demonstrate for the multiple-scan receiver, it can easily be shown for the two-scan receiver.

4. FEASIBILITY OF THE TWO-SCAN RECEIVER

By making some appropriate assumptions, and a simplification of the programmed-sweep receiver, it has been possible to obtain some numerical results which indicate the advantage of the programmed-sweep receiver for the two-scan case.

A quantized program function was chosen. The scaling was selected on the basis of Figs. 5 through 9 to yield a high probability of intercept for input signal-to-noise ratios of 10 and higher. Furthermore, it is assumed in the performance calculations that the intercept probability for this program function is so close to unity that the signal frequency will always be contained in the rescan band. The program function is shown in Fig. 15. Figures 16 and 17 show the relation of this program function to the photographic records of Figs. 6b and 8b for V_c = 15 volts. Note that the program function incorporates the test of signal present on every scan, providing for receiver recovery after

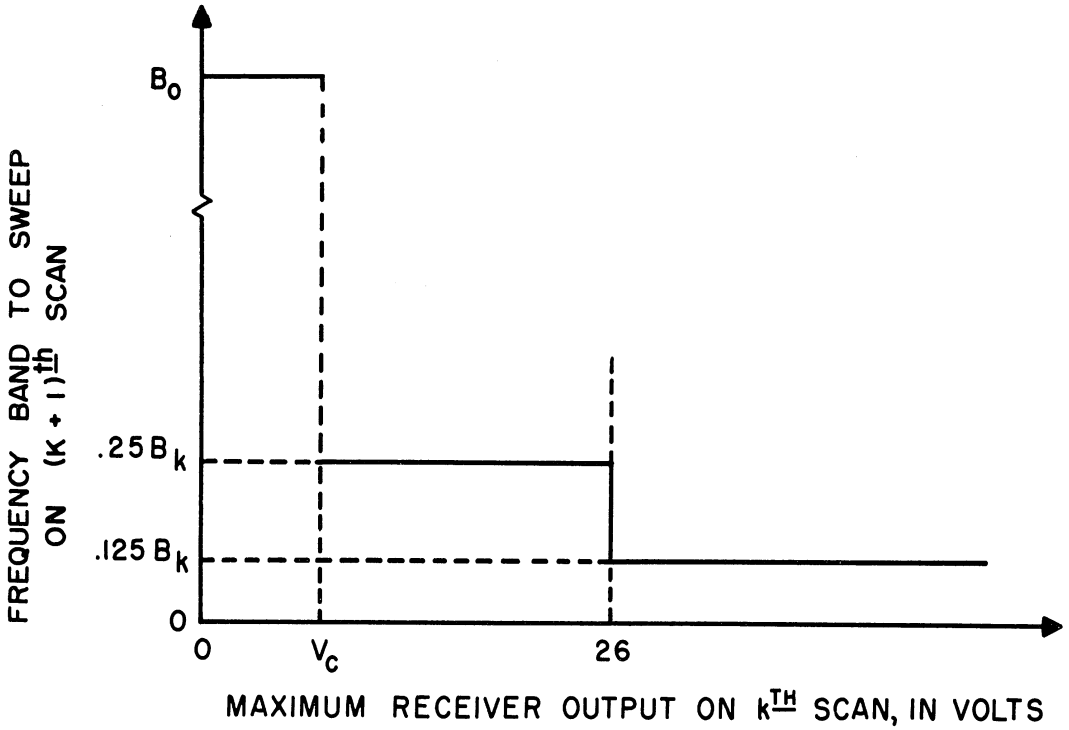

Fig. 15. Program Function for the Two-Scan Receiver

a detection failure. Since the intercept probability is assumed to be unity, degradation of the frequency identification performance results only from detection failures, i.e., situations in which the receiver fails to detect the presence of the signal in the band swept.

This analysis will be limited to a constant sweep-time receiver which makes two scans through the signal frequency. The performance of the two-scan receiver will be compared with that of a relatively slow-scan receiver, where the scan time of the slow receiver is twice the scan time of the two-scan receiver. Figure 18 illustrates the frequency-time sweep patterns for these two cases.

The comparison of performance will be made for three pairs of conditions on signal-to-noise ratio, S/N, and the normalized scan time, bT_o. The sweep bandwidth of the initial scan, B_o, is constant and equal to 100 times the IF bandwidth, b. The experimental data, which are the

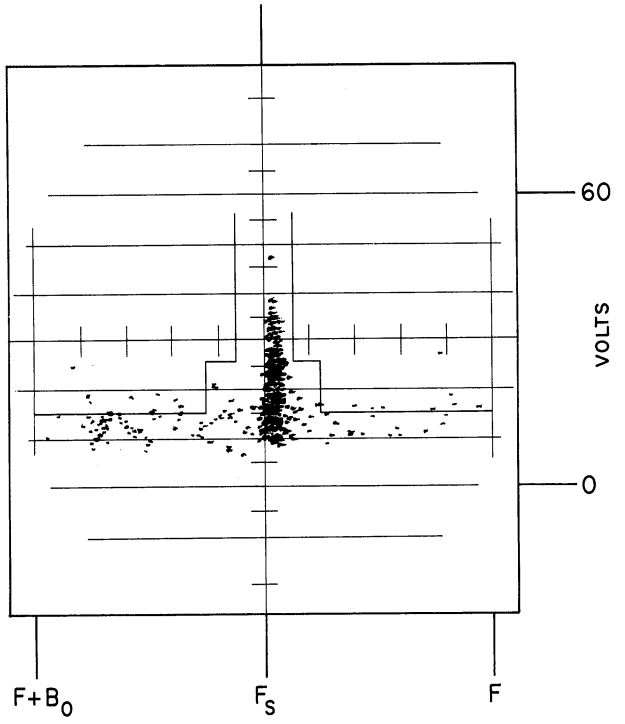

FIG. 16 TWO-SCAN PROGRAM FUNCTION RELATED TO FIG. 6 (b)

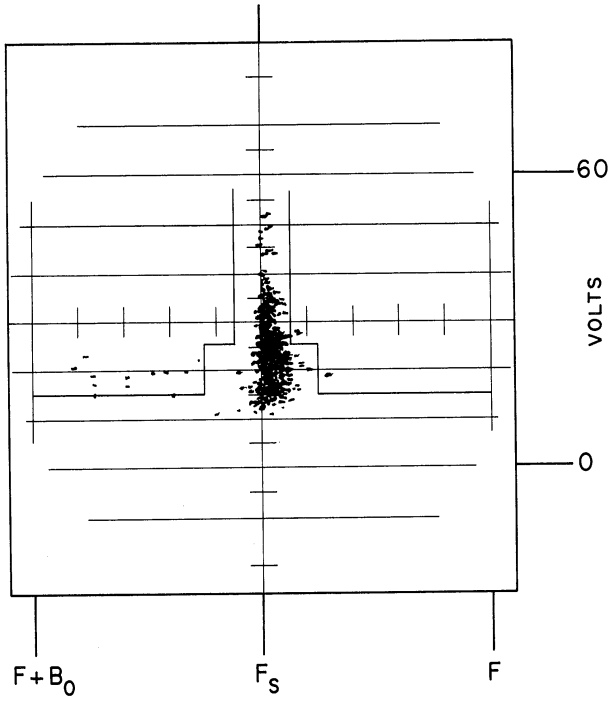

FIG. 17 TWO-SCAN PROGRAM FUNCTION RELATED TO FIG. 8(b)

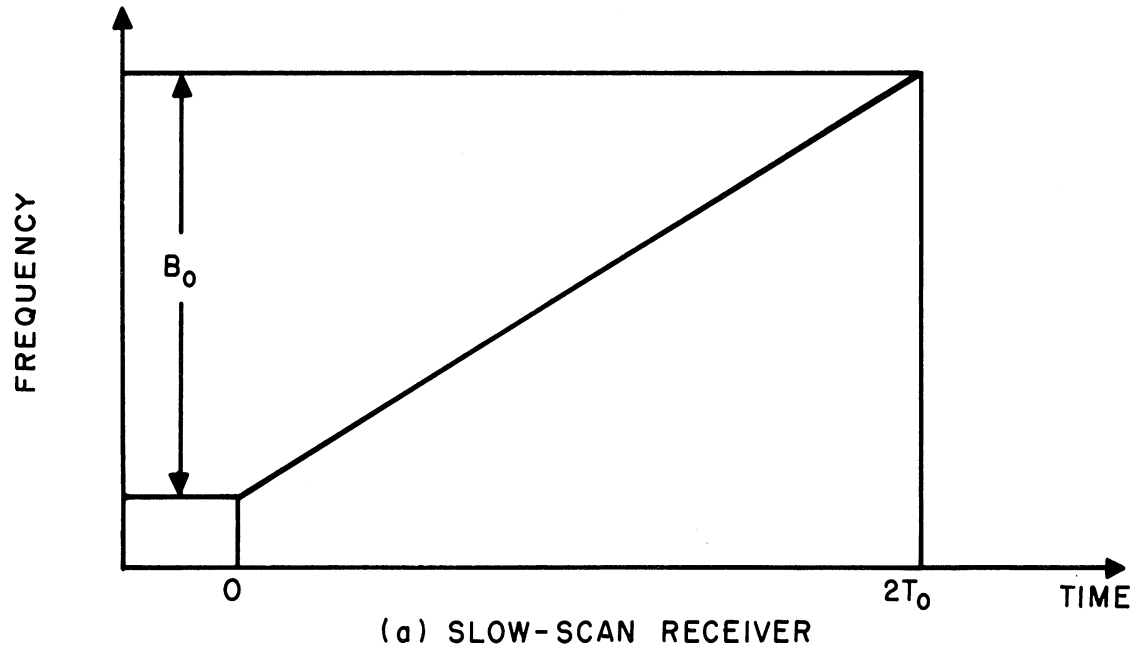

(a) SLOW-SCAN RECEIVER

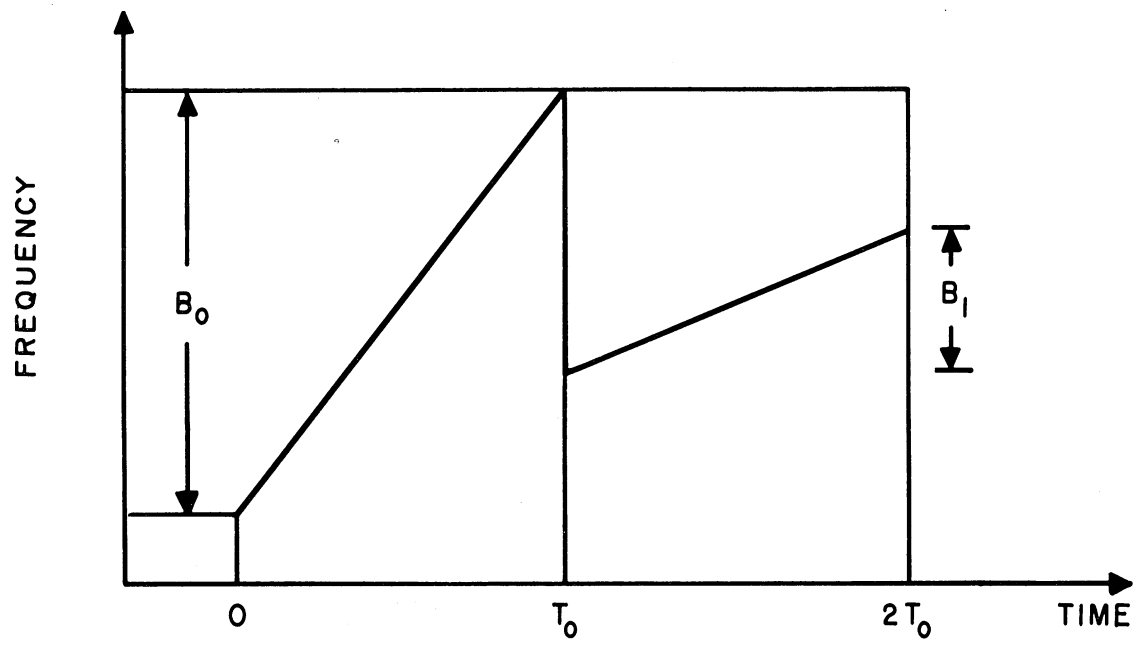

(b) TWO-SCAN RECEIVER

FIG. 18 FREQUENCY-TIME SWEEP PATTERNS FOR THE TWO RECEIVER CASES.

basis of the receiver performance calculation, were obtained from the one-scan panoramic receiver simulation. Since the program function is quantized, the probability distribution functions of the receiver output for the appropriate sweep bandwidth and sweep speed are sufficient to determine the performance. Furthermore, data for the initial sweep bandwidth and the several values of B_1 allowed by the program function are all that is required. Table II gives the values of sweep speed used for these sweep bandwidths and the normalized scan times for which the calculations are made (for the two-scan receiver). The sweep speed values given are those available on the panoramic signal generator which satisfy approximately the sweep bandwidth and scan time conditions. The errors involved in the use of these approximate values do not significantly affect the performance comparison.

TABLE II

SWEEP SPEED VALUES FOR

THE TWO-SCAN RECEIVER

NORMALIZED SWEEP BANDWIDTH	NORMALIZED SWEEP SPEED s/b^2	
B/b	$bT_o = 45$	$bT_o = 90$
100	2.0	1.2
25	0.5	0.3
12.5	0.3	0.15

The performance is judged from two aspects. The receiver operating characteristic (ROC) is used to evaluate performance in regard to detection of the signal presence at $2T_o$. An average frequency resolution, computed for the condition that the presence of the signal has been detected at $2T_o$, is used to evaluate frequency identification performance. Average frequency resolution, as used here, is the average bandwidth determined at $2T_o$ for the next sweep of the receiver.

The receiver operating characteristic (ROC) is a normal-normal plot of the probability of correct signal detection against the probability of false alarm for a range of V_c, the decision threshold value. Since V_c is also a parameter of the program function, the average frequency resolution will vary along the ROC.

Figures 19, 20, and 21 show ROC's for the two-scan and slow-scan receivers with values of frequency resolution marked for the appropriate V_c. The range of V_c is from 12 to 15 volts. The ROC for the slow-scan receiver is directly obtainable from one-scan data; the two-scan ROC is calculated from one-scan data. Appendix B gives the calculations for one set of conditions.

The figures show that frequency resolution is better in the two-scan case for all conditions considered, while the measure of detection performance, d', for equal conditional errors is better for the two-scan receiver, except at the lowest signal-to-noise ratio.

Frequency resolution for the two-scan receiver improves with decreasing V_c, since there is smaller probability of a detection failure (miss) on the first scan. On the other hand, frequency resolution appears

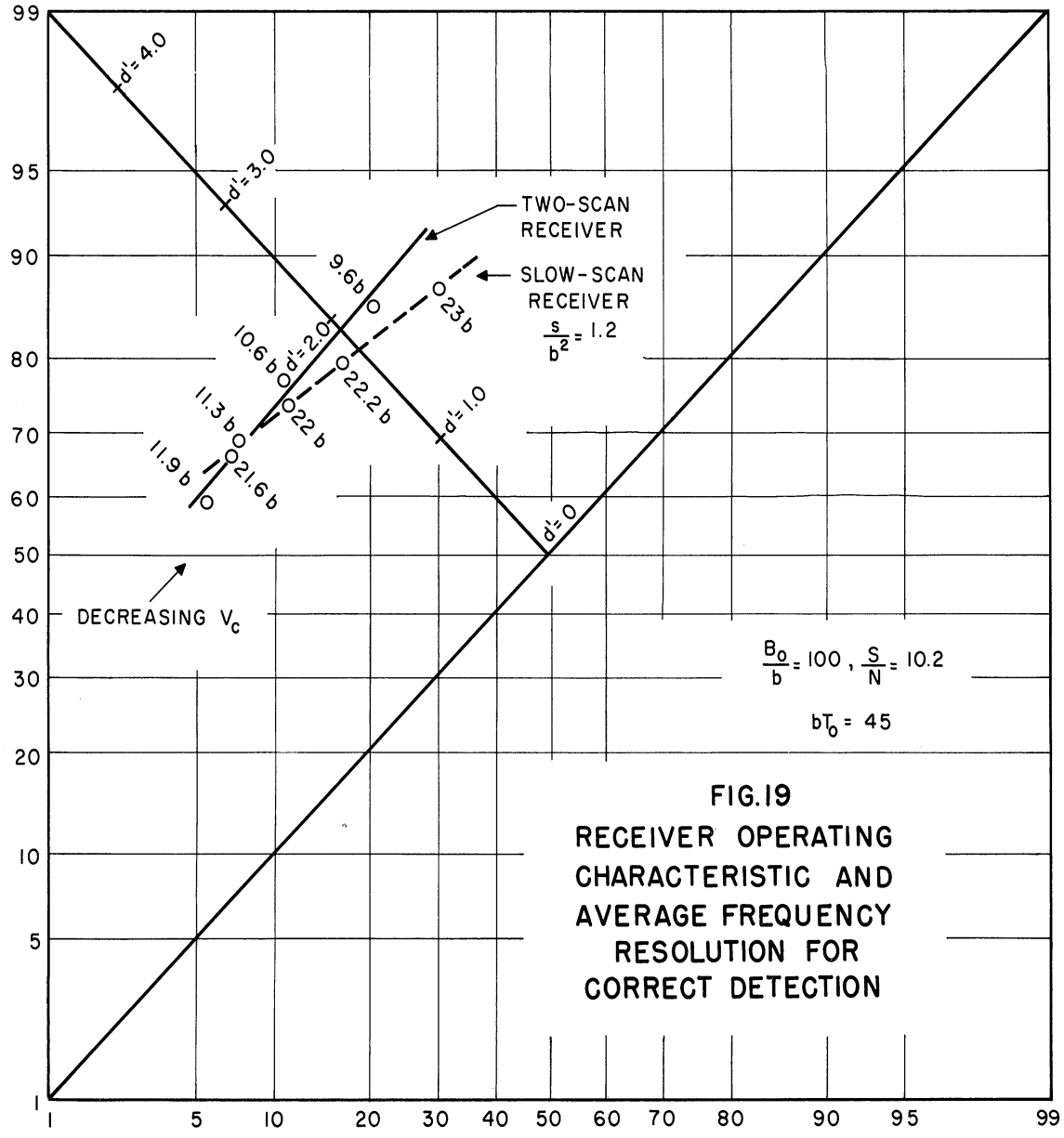

FIG.19
RECEIVER OPERATING CHARACTERISTIC AND AVERAGE FREQUENCY RESOLUTION FOR CORRECT DETECTION

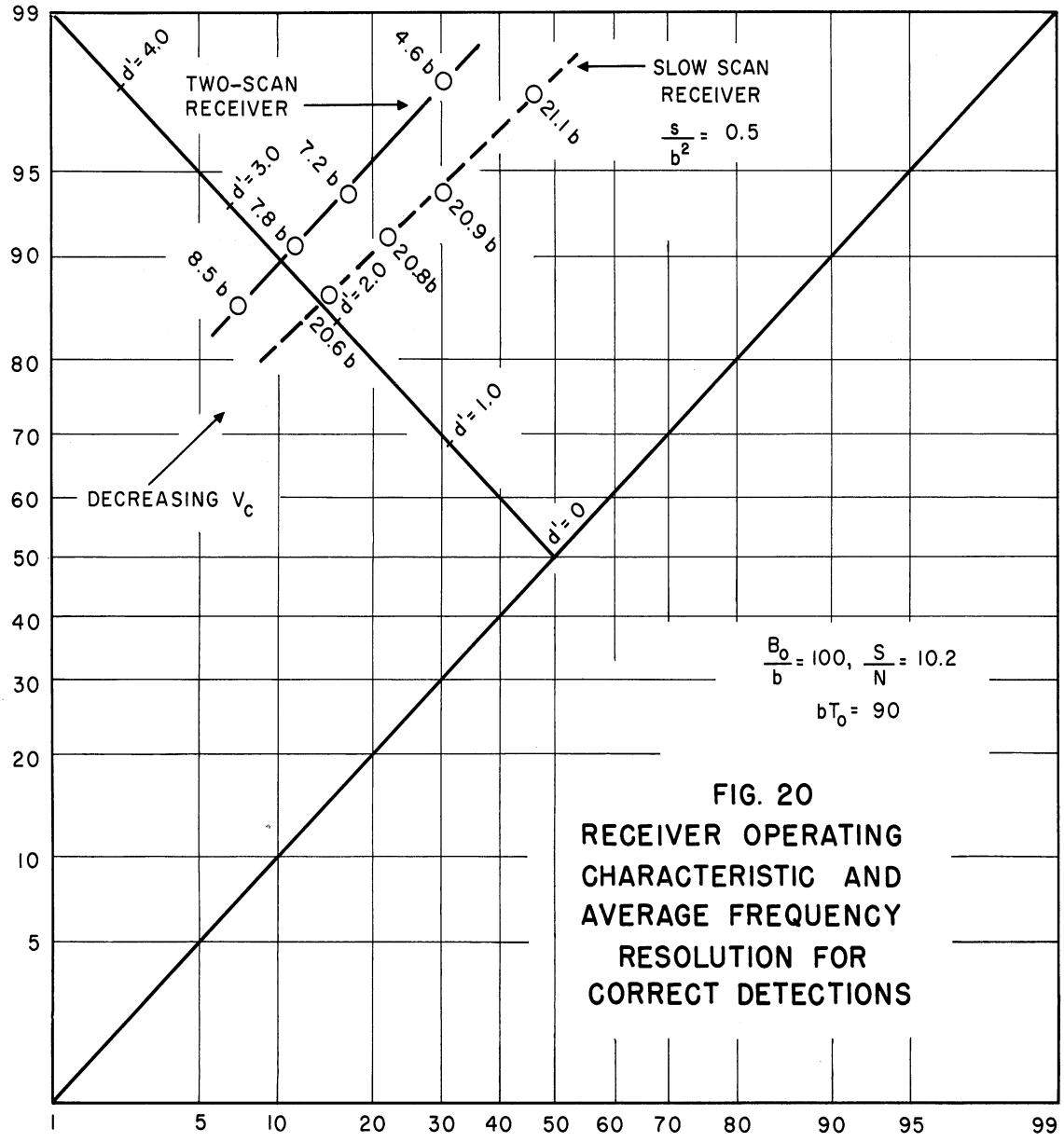

FIG. 20
RECEIVER OPERATING CHARACTERISTIC AND AVERAGE FREQUENCY RESOLUTION FOR CORRECT DETECTIONS

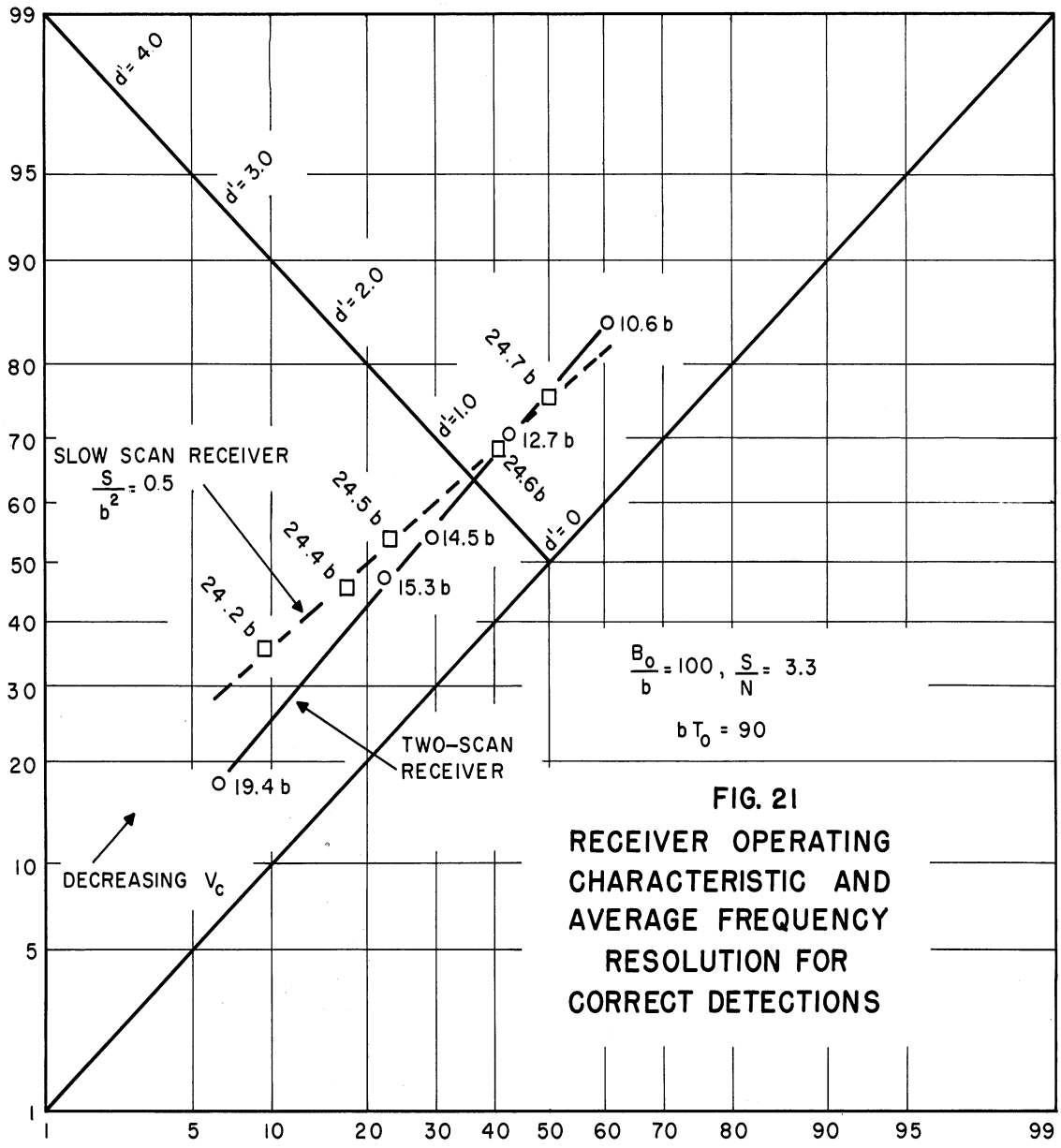

FIG. 21
RECEIVER OPERATING CHARACTERISTIC AND AVERAGE FREQUENCY RESOLUTION FOR CORRECT DETECTIONS

to be worse with decreasing V_c for the slow-scan receiver. This is because frequency resolution is computed only for correct detections. The probability of the slow-scan receiver sweeping 1/4 of the original band on the next scan is therefore increased if V_c is decreased.

It should also be noted that the improvement in performance of the two-scan receiver over the one-scan receiver diminishes as the S/N ratio decreases, or as the sweep speed increases. Thus, it is expected that the two-scan receiver will show relatively better performance as the effective output signal-to-noise ratio increases.

5. SUMMARY

The programmed-sweep receiver is proposed as a signal frequency identification device in applications requiring low search time. The difficulty in designing this receiver lies in finding the sweep bandwidth program function and sweep rate computer which will yield minimum identification time.

The feasibility of the programmed-sweep receiver has been demonstrated for a two-scan receiver by a comparison of the performance with a receiver which makes only one scan in the same time interval. The relative performance of the two-scan receiver improves as the effective output signal-to-noise ratio increases.

APPENDIX A

OPERATION OF HOLDING CIRCUIT

Figure A-1 is the schematic diagram of the holding circuit. To explain its operation, assume an input voltage waveform as shown in Fig. A-2a, and consider what occurs up to a very short time after the first peak of the input.

The 5μf capacitor C1 is charged through the first cathode follower and vacuum diode to the peak value of the input. The diode prevents discharging of C1 from this value when the input voltage falls. Thus the peak value of the input is held on C1.

As C1 is charging, the 0.5μf capacitor C3 is charging through a resistor network to the value of the B+ supply voltage. By switching resistance values, the time constant of this network can be selected to be much longer than the observation time interval. Thus, the voltage on C3 rises linearly, and its value is proportional to time from the beginning of the observation interval. (When the circuit is used with a constant sweep-speed panoramic receiver, this voltage is also proportional to frequency.) The rising voltage on C3 passes through cathode followers and a vacuum diode and is held on C2.

The 12AX7 differential amplifier and 12AT7 dual cathode followers form a differential switching circuit. While C1 is charging, the cathode of the left half of the 12AT7 (point A in Fig. A-1) is at a large positive voltage, set by the level adjustment. When the peak of the input has been reached and the input voltage begins to fall, the

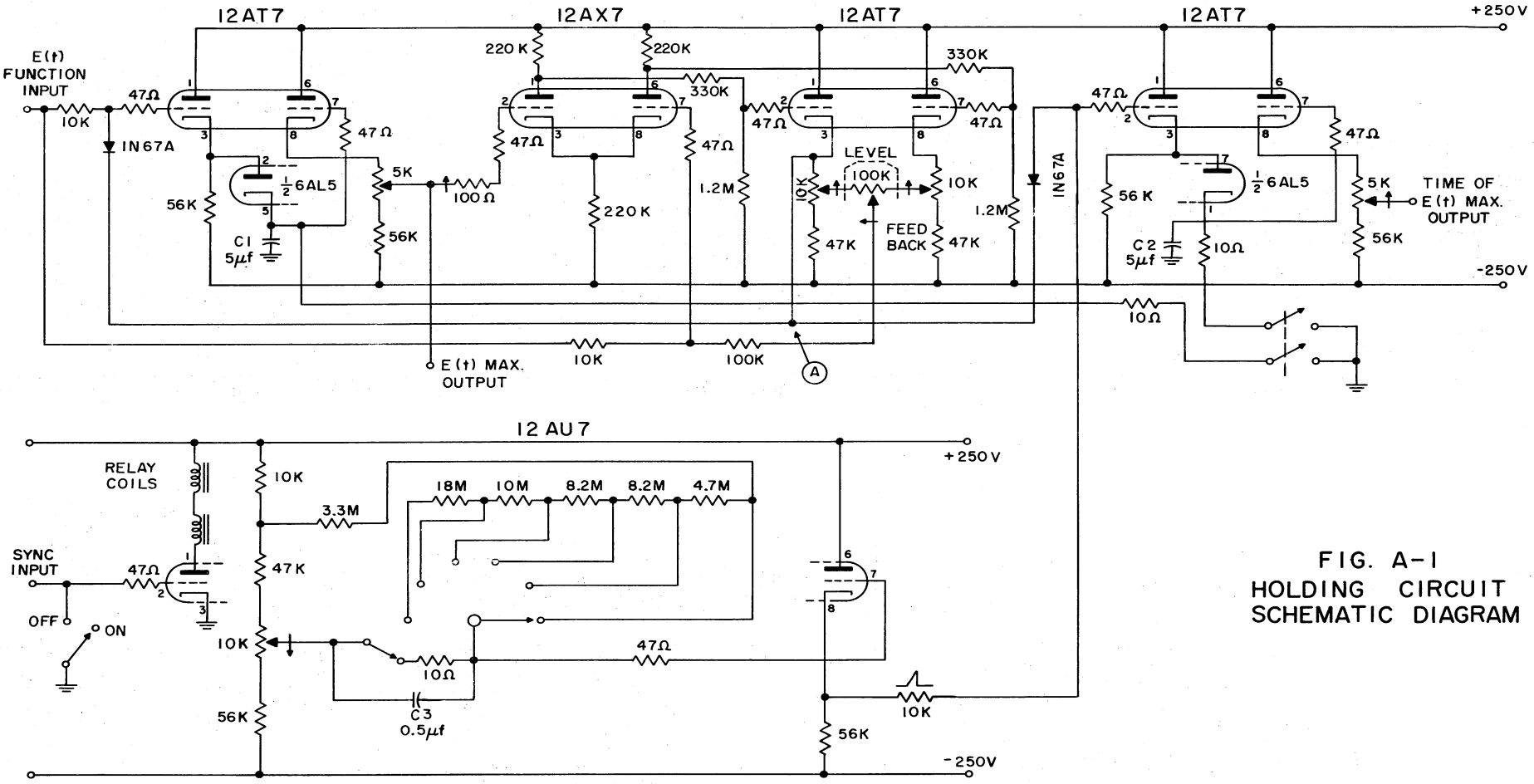

FIG. A-1
HOLDING CIRCUIT
SCHEMATIC DIAGRAM

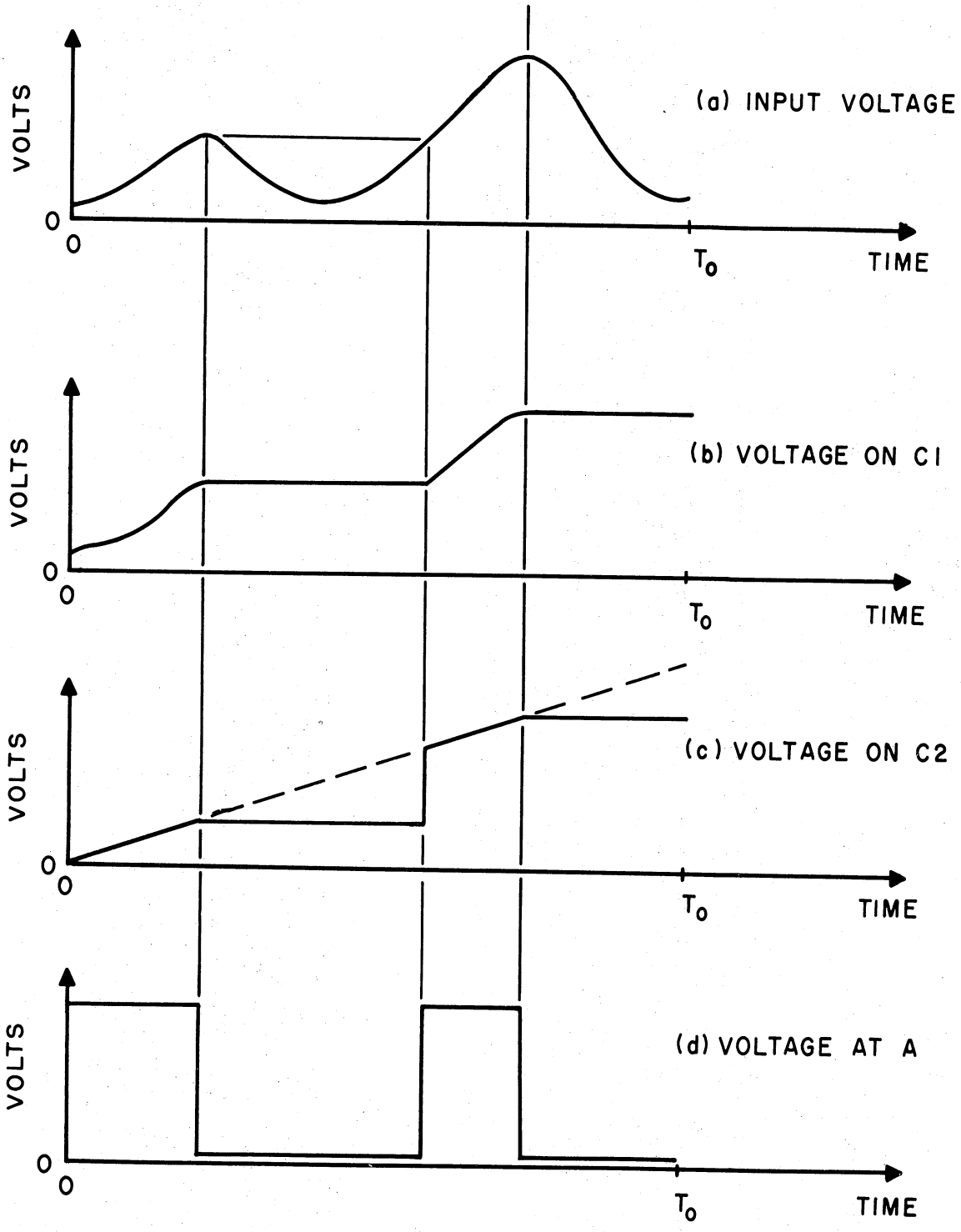

FIG. A-2 HOLDING CIRCUIT WAVEFORMS ILLUSTRATING OPERATION

grid of the right half of the 12AX7 also begins to fall, due to coupling from the input through the 10K resistor. Since there is a common cathode resistor in the differential amplifier, the plate of the left half of the 12AX7 also falls, and the plate-to-grid coupling causes the left cathode of the 12AT7 to fall. The regenerative action provided by positive feedback through the left half of the 12AT7 to the right half of the 12AX7 results in very fast switching of the voltage at A from a large positive value to nearly ground potential. The IN67A diodes conduct, and the rising voltage from C3 is effectively grounded at the point between the two cathode followers. Any further rise of the voltage on C2 is thereby prevented. The diode conduction also grounds the voltage at the grid of the input cathode follower. Figure A-2 illustrates the waveforms in the circuit while the foregoing action is occurring. The voltage at A remains low as long as the input voltage is lower than the voltage held on C1.

Consider now what happens when the input voltage rises above the value of the first peak. Since the grid voltage of the input cathode follower is effectively grounded through the crystal diode, the voltage on C1 cannot, for the moment, rise above the value of the first peak. Hence, as the input voltage rises above this value, the plate of the left half of the 12AX7 begins to rise. The regenerative action described previously quickly brings the cathode voltage at A back up to a large positive value, unclamping the input cathode follower grid and the rising voltage from C3. C1 charges instantly to the input voltage and the voltage on C2 reverts to what it would have been had the first peak not occurred. When the next peak occurs, the switching proceeds as described before. Now,

however, the voltage held on C2 is larger, reflecting the later time occurrence of the second peak, and the voltage on C1 is the voltage value of the second peak. The voltages on C1 and C2, properly isolated by cathode followers, are the outputs of the holding circuit.

The circuit is presently designed to use a sync voltage which falls, at the start of the observation interval, from ground potential to a value sufficiently negative to cut off the half of the 12AU7 controlling the relays. At the end of the observation interval, when the sync voltage returns to ground, the relays are energized, discharging the holding capacitors and capacitor C3. Ten-ohm resistors are used in the discharge circuits to prevent damage to the relay contacts due to arcing.

APPENDIX B

ILLUSTRATIVE CALCULATIONS OF TWO-SCAN RECEIVER PERFORMANCE

Let the following conditions apply on the initial sweep:

band swept, B_o = 100b

sweep rate (normalized), s/b^2 = 1.2 for the two-scan receiver

sweep rate (normalized), s/b^2 = 0.5 for the one-scan receiver

input S/N = 10.2 on every sweep.

Then the program function, Fig. 15, will allow the two-scan receiver to sweep bandwidths B_1 = 100b, 25b, 12.5b on the second scan (first re-scan), depending upon the maximum output amplitude. At the end of the second scan, the band defined for the next scan may be one of the values, B_2 = 100b, 25b, 12.5b, 6.25b, 3.125b, 1.563b.

If the maximum receiver output, in volts, on the kth sweep is X_k, the probability of the band swept on the next sweep is as follows:

$$P_{B_k}(B_{k+1} = B_o) = P_{B_k}(X_k < V_c) = 1-P_{B_k}(X_k > V_c) \quad (k=0,1)$$

$$P_{B_k}(B_{k+1} = .25B_m) = P_{B_k}(V_c < X_k < 26) = P_{B_k}(X_k > V_c) - P_{B_k}(X_k > 26)$$

$$P_{B_k}(B_{k+1} = .125\,B_m) = P_{B_k}(X_k > 26)$$

The probability distribution functions of the receiver output for the appropriate bandwidth and sweep rate are all that is required for the

calculations. Also, since B_2 can be computed from the receiver output when B_1 is the sweep band, the distribution functions for bandwidths 100b, 25b, 12.5b are sufficient. The receiver scan time is constant, so the sweep rate must decrease by the same factor as the sweep band when the receiver makes the next scan. Tables B-I and B-II give the probability distribution functions for the conditions of interest. These were obtained from the one-scan receiver simulation. Tables B-III and B-IV give the false alarm probabilities. Since the two-scan receiver sweeps in equal time intervals, the false alarm probability on any sweep is the same as on the initial sweep.

TABLE B-I

PROBABILITY DISTRIBUTION FUNCTIONS FOR TWO-SCAN RECEIVER OUTPUT, SIGNAL PRESENT

(a) B = 100b, s/b^2 = 1.2

V (volts)	12	13	14	15	26
$P(X_k > V)$	.872	.794	.742	.666	.176

(b) B = 25b, s/b^2 = 0.3

V (volts)	12	13	14	15	26
$P(X_k > V)$	.994	.966	.954	.938	.512

(c) B = 12.5b, s/b^2 = 0.15

V (volts)	12	13	14	15	26
$P(X_k > V)$	1	1	.998	.998	.798

TABLE-II

PROBABILITY DISTRIBUTION FUNCTION FOR
ONE-SCAN RECEIVER, SIGNAL PRESENT

$B = 100b, \quad s/b^2 = 0.5$

V (volts)	12	13	14	15	26
$P(X_k > V)$	.976	.940	.916	.864	.304

TABLE B-III

FALSE ALARM PROBABILITIES FOR
TWO-SCAN RECEIVER

V (volts)	12	13	14	15	26
$P(X_k > V)$	.302	.170	.112	.072	0

TABLE B-IV

FALSE ALARM PROBABILITIES FOR
ONE-SCAN RECEIVER

V (volts)	12	13	14	15	26
$P(X_k > V)$	.365	.234	.177	.121	.002

To illustrate the computation, take $V_c = 14$ volts, and consider first the two scan receiver.

$B_k = B_o = 100b$

$$P_{B_o}(B_1 = 100b) = 1-P(X_k > 14) = .258$$
$$P_{B_o}(B_1 = 25b) = P(X_k > 14) - P(X_k > 26) = .566$$
$$P_{B_o}(B_1 = 12.5b) = P(X_k > 26) = .176$$

$B_k = B_1 = 100b$

$$P_{B_1}(B_2 = 100b) = .258$$
$$P_{B_1}(B_2 = 25b) = .566$$
$$P_{B_1}(B_2 = 12.5b) = .176$$

$B_k = B_1 = 25b$

$$P_{B_1}(B_2 = 100b) = .046$$
$$P_{B_1}(B_2 = 6.25b) = .442$$
$$P_{B_1}(B_2 = 3.125b) = .512$$

$B_k = B_1 = 12.5b) = .798$

$$P_{B_1}(B_2 = 100b) = .002$$
$$P_{B_1}(B_2 = 3.125b) = .200$$
$$P_{B_1}(B_2 = 1.563b) = .798$$

The average frequency resolution is the average of B_2, conditional to a detection of the signal on the second scan ($B_2 \neq 100b$). So,

$$\text{Average frequency resolution} = \frac{\sum_{\text{all } B_2 \neq 100b} B_2 \, P_{B_o}(B_2)}{P_{B_o}(B_2 \neq 100b)} \qquad \text{(B-1)}$$

$P_{B_o}(B_2 \neq 100b)$ is the two-scan probability of signal detection,

$$P_2(D) = \sum_{\text{all } B_1} P_{B_o}(B_1) \, P_{B_1}(D), \qquad \text{(B-2)}$$

and, for this case,

$$P_2(D) = (0.566)(0.954) + (0.176)(0.998) + (0.258)(0.742) = 0.909$$

Note that $P_2(D)$ and the corresponding false alarm probability from Table B-III represent one point on the ROC for the two-scan receiver.

Now, the calculation of

$$\sum_{\text{all } B_2 \neq 100b} B_2 P_{B_o}(B_2) = \sum_{\text{all } B_2 \neq 100b} B_2 \sum_{\text{all } B_1} P_{B_o}(B_1) \cdot P_{B_1}(B_2) \qquad \text{(B-3)}$$

can be carried out systematically using the tabulation shown below, where the entries in the top array are the values $P_{B_o}(B_1) \cdot P_{B_1}(B_2)$.

		B_1		
		100b	25b	12.5b
B_2	25 b	.1465	-	-
	12.5 b	.0454	-	-
	6.25 b	-	.2510	-
	3.125b	-	.2908	.0352
	1.563b	-	-	.1404

$\sum_{B_1} P_{B_o}(B_1) \cdot P_{B_1}(B_2)$
.1465
.0454
.2510
.3260
.1404

$B_2 \sum_{B_1} P_{B_o}(B_1) \cdot P_{B_1}(B_2)$
3.66 b
.56 b
1.57 b
1.02 b
.22 b

$$\sum_{\text{all } B_2 \neq 100b} B_2 \sum_{\text{all } B_1} P_{B_o}(B_1) \cdot P_{B_1}(B_2) = \boxed{7.03\ b}$$

Then,

$$\text{Average frequency resolution} = \frac{7.03b}{0.909} = 7.84b.$$

For the one-scan receiver the same program function is used, and the probabilities are

$$P_{B_o}(B_1 = 100b) = 1-0.940 = 0.060$$

$$P_{B_o}(B_1 = 25b) = 0.940-0.304 = 0.636$$

$$P_{B_o}(B_1 = 12.5b) = 0.304$$

The average frequency resolution of the one-scan receiver is the average of B_1, conditional to signal detection on the first scan. So,

$$\text{Average frequency resolution} = \frac{\sum_{\text{all } B_1 \neq 100b} B_1 P_{B_o}(B_1)}{P_{B_o}(B_1 \neq 100b)},$$

and this calculation is simply

$$\text{Average frequency resolution} = \frac{(25b)(0.636) + (12.5b)(0.304)}{0.940} = 21b.$$

Also, $P_{B_o}(X_m > V_c) = 0.940$, and $P_{B_o}(FA) = 0.177$, from Table B-IV, represent the point on the ROC.

The receiver operating characteristic of Fig. 18 is found by proceeding through the foregoing calculations for other values of V_c.

REFERENCES

1. H. W. Batten, R. A. Jorgensen, A. B. Macnee, and W. W. Peterson, "The Response of a Panoramic Receiver to CW and Pulse Signals," Technical Report No. 3, Electronic Defense Group, University of Michigan Research Institute, June 1952.
2. Q. C. Wilson, II and D. W. Fife, "Statistical Measurements of the Detection of a Continuous Signal by a Panoramic Receiver," Technical Report No. 105, Electronic Defense Group, University of Michigan Research Institute, May 1960.
3. W. P. Tanner, Jr., and T. G. Birdsall, "Definitions of d' and η as Psychophysical Measures," Technical Report No. 80, Electronic Defense Group, University of Michigan Research Institute, February 1958.

DISTRIBUTION LIST

Copy No.	
1-2	Commanding Officer, U. S. Army Signal Research and Development Laboratory, Fort Monmouth, New Jersey, ATTN: Senior Scientist, Countermeasures Division
3	Commanding General, U. S. Army Electronic Proving Ground, Fort Huachuca, Arizona, ATTN: Director, Electronic Warfare Department
4	Chief, Research and Development Division, Office of the Chief Signal Officer, Department of the Army, Washington 25, D. C., ATTN: SIGEB
5	Chief, Plans and Operations Division, Office of the Chief Signal Officer, Washington 25, D. C., ATTN: SIGEW
6	Commanding Officer, Signal Corps Electronics Research Unit, 9560th USASRU, P. O. Box 205, Mountain View, California
7	U. S. Atomic Energy Commission, 1901 Constitution Avenue, N.W., Washington 25, D. C., ATTN: Chief Librarian
8	Director, Central Intelligence Agency, 2430 E Street, N.W., Washington 25, D. C., ATTN: OCD
9	Signal Corps Liaison Officer, Lincoln Laboratory, Box 73, Lexington 73, Massachusetts, ATTN: Col. Clinton W. Janes
10-19	Commander, Armed Services Technical Information Agency, Arlington Hall Station, Arlington 12, Virginia
20	Commander, Air Research and Development Command, Andrews Air Force Base, Washington 25, D. C., ATTN: RDTC
21	Directorate of Research and Development, USAF, Washington 25, D. C., ATTN: Chief, Electronic Division
22	Commander, Wright Air Development Center, Wright-Patterson Air Force Base, Ohio, ATTN: WCOSI-3
23	Commander, Wright Air Development Center, Wright-Patterson Air Force Base, Ohio, ATTN: WWRNGW-1
24	Commander, Wright Air Development Center, Wright-Patterson Air Force Base, Ohio, ATTN: WCLGL-7
25	Commander, Air Force Cambridge Research Center, L. G. Hanscom Field, Bedford, Massachusetts, ATTN: CROTLR-2
26	Commander, Rome Air Development Center, Griffiss Air Force Base, New York, ATTN: RCSSLD
27	Commander, Air Proving Ground Center, ATTN: Adj/Technical Report Branch, Eglin Air Force Base, Florida
28	Commander, Special Weapons Center, Kirtland Air Force Base, Albuquerque, New Mexico
29	Chief, Bureau of Ordnance, Code ReO-1, Department of the Navy, Washington 25, D. C.
30	Chief of Naval Operations, EW Systems Branch, OP-347, Department of the Navy, Washington 25, D. C.
31	Chief, Bureau of Ships, Code 840, Department of the Navy, Washington 25, D. C.
32	Chief, Bureau of Ships, Code 843, Department of the Navy, Washington 25, D. C.
33	Chief, Bureau of Aeronautics, Code EL-8, Department of the Navy, Washington 25, D. C.
34	Commander, Naval Ordnance Test Station, Inyokern, China Lake, California, ATTN: Test Director-Code 30
35	Commander, Naval Air Missile Test Center, Point Mugu, California, ATTN: Code 366
36	Director, Naval Research Laboratory, Countermeasures Branch, Code 5430, Washington 25, D. C.
37	Director, Naval Research Laboratory, Washington 25, D. C., ATTN: Code 2021
38	Director, Air University Library, Maxwell Air Force Base, Alabama, ATTN: CR-4987
39	Commanding Officer-Director, U. S. Naval Electronic Laboratory, San Diego 52, California
40	Office of the Chief of Ordnance, Department of the Army, Washington 25, D. C., ATTN: ORDTU
41	Chief, West Coast Office, U. S. Army Signal Research and Development Laboratory, Bldg. 6, 75 S. Grand Avenue, Pasadena 2, California
42	Commanding Officer, U. S. Naval Ordnance Laboratory, Silver Springs 19, Maryland

DISTRIBUTION LIST (Cont'd)

Copy No.	
43-44	Chief, U. S. Army Security Agency, Arlington Hall Station, Arlington 12, Virginia, ATTN: GAS-24L
45	President, U. S. Army Defense Board, Headquarters, Fort Bliss, Texas
46	President, U. S. Army Airborne and Electronics Board, Fort Bragg, North Carolina
47	U. S. Army Antiaircraft Artillery and Guided Missile School, Fort Bliss, Texas, ATTN: E & E Department
48	Commander, USAF Security Service, San Antonio, Texas, ATTN: CLR
49	Chief of Naval Research, Department of the Navy, Washington 25, D. C., ATTN: Code 931
50	Commanding Officer, U. S. Army Security Agency, Operations Center, Fort Huachuca, Arizona
51	President, U. S. Army Security Agency Board, Arlington Hall Station, Arlington, 12, Virginia
52	Operations Research Office, Johns Hopkins University, 6935 Arlington Road, Bethesda 14, Maryland, ATTN: U. S. Army Liaison Officer
53	The Johns Hopkins University, Radiation Laboratory, 1315 St. Paul Street, Baltimore 2, Maryland, ATTN: Librarian
54	Stanford Electronics Laboratories, Stanford University, Stanford, California, ATTN: Applied Electronics Laboratory Document Library
55	HRB-Singer, Inc., Science Park, State College, Penn., ATTN: R. A. Evans, Manager, Technical Information Center
56	ITT Laboratories, 500 Washington Avenue, Nutley 10, New Jersey, ATTN: Mr. L. A. DeRosa, Div. R-15 Lab.
57	The Rand Corporation, 1700 Main Street, Santa Monica, California, ATTN: Dr. J. L. Hult
58	Stanford Electronics Laboratories, Stanford University, Stanford, California, ATTN: Dr. R. C. Cumming
59	Willow Run Laboratories, The University of Michigan, P. O. Box 2008, Ann Arbor Michigan, ATTN: Dr. Boyd
60	Stanford Research Institute, Menlo Park, California, ATTN: Dr. Cohn
61-62	Commanding Officer, U. S. Army Signal Missile Support Agency, White Sands Missile Range, New Mexico, ATTN: SIGWS-EW and SIGWS-FC
63	Commanding Officer, U. S. Naval Air Development Center, Johnsville, Pennsylvania, ATTN: Naval Air Development Center Library
64	Commanding Officer, U. S. Army Signal Research and Development Laboratory, Fort Monmouth, New Jersey, ATTN: U. S. Marine Corps Liaison Office, Code AO-4C
65	President U. S. Army Signal Board, Fort Monmouth, New Jersey
66-76	Commanding Officer, U. S. Army Signal Research and Development Laboratory, Fort Monmouth, New Jersey ATTN: 1 Copy - Director of Research 1 Copy - Technical Documents Center ADT/E 1 Copy - Chief, Ctms Systems Branch, Countermeasures Division 1 Copy - Chief, Detection & Location Branch, Countermeasures Division 1 Copy - Chief, Jamming & Deception Branch, Countermeasures Division 1 Copy - File Unit No. 4, Mail & Records, Countermeasures Division 1 Copy - Chief, Vulnerability Br., Electromagnetic Environment Division 1 Copy - Reports Distribution Unit, Countermeasures Division File 3 Cpys - Chief, Security Division (for retransmittal to BJSM)
77	Director, National Security Agency, Ft. George G. Meade, Maryland, ATTN: TEC
78	Dr. H. W. Farris, Director, Electronic Defense Group, University of Michigan Research Institute, Ann Arbor, Michigan
79-99	Electronic Defense Group Project File, University of Michigan Research Institute, Ann Arbor, Michigan
100	Project File, University of Michigan Research Institute, Ann Arbor, Michigan

Above distribution is effected by Countermeasures Division, Surveillance Dept., USASRDL, Evans Area, Belmar, New Jersey. For further information contact Mr. I. O. Myers, Senior Scientist, telephone PRospect 5-3000, Ext. 61252.